



Peer review status:

This is a non-peer-reviewed preprint submitted to EarthArXiv.

Quantum Entropy and Probabilistic Clustering for Uncertainty-Aware Groundwater Quality Assessment in Geochemically Complex Terrains of Eastern India

Author: Tapas Ranjan Patra

Assistant Professor, Department of Geography

Rajendra University, Balangir, 767002, Odisha

Email: tapasranjan05@outlook.com

Abstract

Groundwater quality assessment in geochemically heterogeneous regions is often constrained by deterministic models that overlook spatial variability, inter-parameter dependencies, and system uncertainty. This study proposes a novel Quantum Entropy-based Groundwater Quality Index (QEGWI), which leverages von Neumann entropy derived from quantum density matrices to weight hydrogeochemical parameters based on multivariate uncertainty dynamically. Applied to a five-year dataset from 1,280 monitoring sites across Odisha, India, QEGWI demonstrated superior sensitivity, spatial resolution, and robustness compared to conventional and Shannon entropy-based indices. Sensitivity analysis revealed fluoride (F^-) and sodium (Na^+) as the dominant pollutants (Sobol index > 0.35), while Monte Carlo simulations confirmed model stability ($\sigma \pm 0.14$). To complement this, a Quantum Probabilistic Clustering (QPC) framework was introduced, modelling groundwater sites as quantum states and utilising fidelity-based soft classification. Five risk-based clusters were identified with high intra-cluster coherence (fidelity > 0.85) and transitional zones showing uncertainty > 0.25 . Together, QEGWI and QPC offer a scalable, uncertainty-aware framework that bridges quantum information theory with environmental risk assessment for hydro geologically complex systems.

Key Words: *Quantum Entropy, Groundwater Quality Assessment, Quantum Probabilistic Clustering, Hydrogeochemical Risk Zonation*

1. INTRODUCTION

Groundwater constitutes a critical component of the global freshwater supply, supporting domestic consumption, agriculture, and industry, especially in arid and semi-arid regions (Scanlon et al., 2023). However, its quality is increasingly compromised due to both natural and anthropogenic influences. Climate change has led to erratic precipitation, prolonged droughts, and declining recharge rates, all of which strain groundwater reserves and exacerbate contamination risks (Barbieri et al., 2023; Panday et al., 2025). Agricultural intensification and industrial expansion contribute to elevated concentrations of nitrates, heavy metals, and persistent organic pollutants (Zhang et al., 2024). Urbanization and changing land use patterns further degrade aquifer health through surface runoff, sewage seepage, and unregulated waste disposal (Sridhar & Parimalarenganayaki, 2024). Natural processes like mineral dissolution, geochemical transformations, and salinity intrusion in coastal areas compound these pressures, making groundwater quality monitoring more complex and essential than ever (Salh et al., 2025).

India's diverse physiographic divisions present unique and region-specific groundwater quality challenges. In the Himalayan region, unregulated mining and fertilizer use increase contamination risks (Mir, 2025). The Indo-Gangetic plains face alarming levels of overextraction, leading to water table depletion and salinity imbalances (MacDonald et al., 2016). Coastal zones are increasingly affected by seawater intrusion, especially where groundwater withdrawal outpaces natural recharge (El Shinawi et al., 2022). The Deccan Plateau, characterized by crystalline rock formations, exhibits naturally occurring contaminants like fluoride and arsenic in alarming concentrations (Jha & Tripathi, 2021).

Odisha, situated along the eastern coast of India, presents a particularly complex case of groundwater management due to its physiographic and climatic variability. The state comprises rolling uplands, fertile coastal plains, and hard rock plateau regions—each with distinct hydrogeological characteristics. In the uplands, seasonal water scarcity and depth fluctuations are common. The coastal areas are vulnerable to saltwater intrusion (Mohanty & Rao, 2019), especially during periods of reduced recharge. The plateau regions, particularly in western and central Odisha, are prone to high fluoride concentrations (Sahu et al., 2021), which pose serious public health risks. Increasing pressure from agriculture, population growth, and industrialization has further strained groundwater quality, with several districts reporting rising levels of contamination in well samples.

Groundwater quality assessment has traditionally relied on Water Quality Index (WQI) models, including NSF-WQI, CWQI, and WAWQI, which aggregate multiple physicochemical

parameters into a single score using fixed or expert-derived weights (Zare et al., 2025). Multivariate statistical techniques like Principal Component Analysis (PCA) (Patel et al., 2024) and Factor Analysis (FA) (Sartirana et al., 2025) have been widely used for dimensionality reduction and pollution source identification. Multi-Criteria Decision Analysis (MCDA) (Dai et al., 2025; Srivastava et al., 2024) approaches, particularly Analytic Hierarchy Process (AHP) (Loganathan & Sathiyamoorthy, 2024) and Technique for Order Preference by Similarity to Ideal Solution (TOPSIS) (Dehghan Rahimabadi et al., 2024), have also been applied for parameter weighting in groundwater studies. Geostatistical interpolation techniques like Inverse Distance Weighting (IDW), Kriging, and Spline (A. Y. Ahmad et al., 2021) are frequently employed for spatial mapping of groundwater quality. More recently, Machine Learning (ML) models, including Random Forest (RF), Support Vector Machines (SVM), Artificial Neural Networks (ANN), and Gradient Boosting Machines (GBM) (Karunanidhi et al., 2025; Singha et al., 2021) have gained prominence due to their ability to capture complex nonlinear relationships. Hybrid approaches integrating fuzzy logic (Abidi et al., 2024; Kisi et al., 2019), and machine learning–statistical methods (Abu et al., 2024; Judeh et al., 2022) also been explored to enhance modelling of groundwater hydrogeochemical interactions.

Despite their widespread use, Traditional WQI models lack adaptability to site-specific hydro chemical variability and ignore parameter interdependencies. These approaches, although effective, often introduce subjectivity in weight assignment and rely on assumptions of data linearity and normality. Geostatistical techniques assume homogeneity and isotropy, which are rarely valid in heterogeneous regions. ML models, while accurate, often behave as black-box systems, requiring large, balanced datasets and offering limited interpretability regarding uncertainty and spatial heterogeneity. Hybrid models, although flexible, demand extensive calibration, expert input, and computational resources, limiting their applicability in routine groundwater quality monitoring.

Entropy-based weighting methods, particularly Shannon entropy, have gained prominence in groundwater quality assessment frameworks. Shannon entropy enables objective determination of parameter weights based on variability and informational content, reducing reliance on subjective expert judgment. Several studies (S. Ahmad et al., 2024; Amiri et al., 2014; Vesković et al., 2024) have incorporated Shannon entropy into Water Quality Index (WQI) models to enhance transparency and minimize bias. However, conventional Shannon entropy primarily addresses individual parameter variability and does not fully capture multivariate dependencies, limiting its effectiveness in complex, heterogeneous groundwater systems. Thus,

while entropy-based approaches offer improved transparency, their current formulations fall short of capturing joint parameter behaviour in spatially variable aquifer systems.

Despite significant advancements in groundwater quality assessment, most existing models fundamentally operate under deterministic assumptions. These models generate fixed outputs solely based on input datasets, without addressing the uncertainties intrinsic to groundwater systems, including measurement errors, sampling variability, and hydro chemical fluctuations. The absence of uncertainty representation critically undermines the reliability of assessments.

Sensitivity to input data further exacerbates this issue. Minor inconsistencies in sampling, measurement, or parameter selection disproportionately influence groundwater quality indices and classification outcomes, compromising the robustness and credibility of results. Additionally, traditional modelling frameworks often fail to capture the spatial heterogeneity that characterizes groundwater systems shaped by variable geology, land use, and anthropogenic pressures.

Recent groundwater quality studies have increasingly attempted to incorporate uncertainty quantification through external methods such as Monte Carlo simulation (Sany et al., 2025) and bootstrapping (Thanh et al., 2024). Although these approaches improve risk evaluation by providing probabilistic ranges around model outputs, they treat uncertainty as a post-processing layer rather than integrating it within the core modelling structure. Consequently, groundwater quality assessments largely remain deterministic, limiting their capacity to reflect complex, variable real-world conditions.

The groundwater scenario in Odisha exemplifies these challenges. The state exhibits pronounced spatial variability across its coastal plains, upland regions, and hard rock plateaus, each marked by distinct hydrogeochemical conditions and varying degrees of anthropogenic stress (Das, 2024; Goswami & Rai, 2024).

Despite extensive groundwater quality studies, no existing research in Odisha has systematically integrated multivariate variability and intrinsic uncertainty within the groundwater quality assessment framework. Previous approaches have primarily focused on static parameter weighting (Ojha et al., 2024), single-year analyses (Jena et al., 2024), and deterministic interpolation (Mahanta & Goswami, 2024), without addressing the probabilistic nature of groundwater systems.

Critically, no study to date has developed a preprocessing framework that inherently captures multivariate groundwater uncertainty globally, without relying on external simulations or post hoc adjustments. The absence of a probabilistic, entropy-driven model that simultaneously

accounts for spatial heterogeneity, parameter interlinkages, and inherent uncertainty represents a foundational gap in groundwater quality assessment.

This study presents a novel groundwater quality assessment framework by incorporating quantum entropy into the formulation of a dynamic Groundwater Quality Index (QEGWI). Unlike conventional weighting approaches, QEGWI leverages von Neumann entropy to encode multivariate dependencies and latent uncertainty within a density matrix structure, enabling adaptive assessment across spatially heterogeneous groundwater systems. Complementing this, a Quantum Probabilistic Clustering (QPC) model is introduced to delineate groundwater risk zones through a probabilistic lens. By representing each site as a quantum state and employing quantum fidelity as a similarity metric, QPC facilitates overlapping cluster memberships, particularly effective in transitional or ambiguous hydrogeochemical contexts. Together, the QEGWI and QPC models offer a cohesive, physically grounded framework. By integrating quantum theory with groundwater assessment, the study provides a flexible, interpretable, and risk-sensitive approach to environmental decision-making.

This study is driven by the following objectives:

- i. To develop a Quantum Entropy-based Groundwater Quality Index (QEGWI) and to apply the QEGWI framework for assessing the groundwater quality of Odisha, and compare the results with established entropy-based methods.
- ii. To introduce a Quantum Probabilistic Clustering (QPC) model that employs quantum fidelity for identifying groundwater risk zones.

By merging quantum entropy with probabilistic clustering, the proposed framework redefines how groundwater quality is assessed and interpreted. It moves beyond traditional scores to offer a scientifically grounded and application-ready tool for risk-based groundwater governance, particularly in spatially complex and data-limited regions like Odisha.

2. MATERIAL AND METHOD

2.1 Study Area

Odisha is located on the eastern coast of India, extending between latitudes 17°49'N and 22°34'N and longitudes 81°27'E and 87°29'E. Covering an area of approximately 155,707 square kilometres (*Fig. 1*). Odisha experiences a tropical monsoon climate characterized by hot summers, high humidity, and concentrated rainfall during the southwest monsoon season from June to September. The state receives an average annual rainfall of around 1450 mm, with

significant spatial variability. Coastal districts tend to receive higher rainfall than inland areas, influencing both recharge rates and groundwater chemistry. The state exhibits complex hydrogeological settings shaped by diverse geological formations. Coastal areas are dominated by alluvial deposits, offering relatively shallow and productive aquifers. In contrast, the central uplands and western plateau regions are underlain by hard rock terrains including granite, gneiss, schist, and basalt. These fractured rock aquifers are generally low in permeability and exhibit significant spatial variability in depth and yield. Both unconfined and semi-confined aquifers are present, with varying vulnerability to contamination depending on lithology and land use.

Groundwater serves as the principal source of irrigation in Odisha, especially in non-monsoon months. Agriculture is predominantly practiced during Kharif and Rabi seasons, with substantial seasonal variation in water demand. Urban and peri-urban areas are increasingly dependent on groundwater for domestic and industrial purposes, further intensifying pressure on aquifer systems. Rapid urbanization in cities has led to increased extraction and localized depletion.

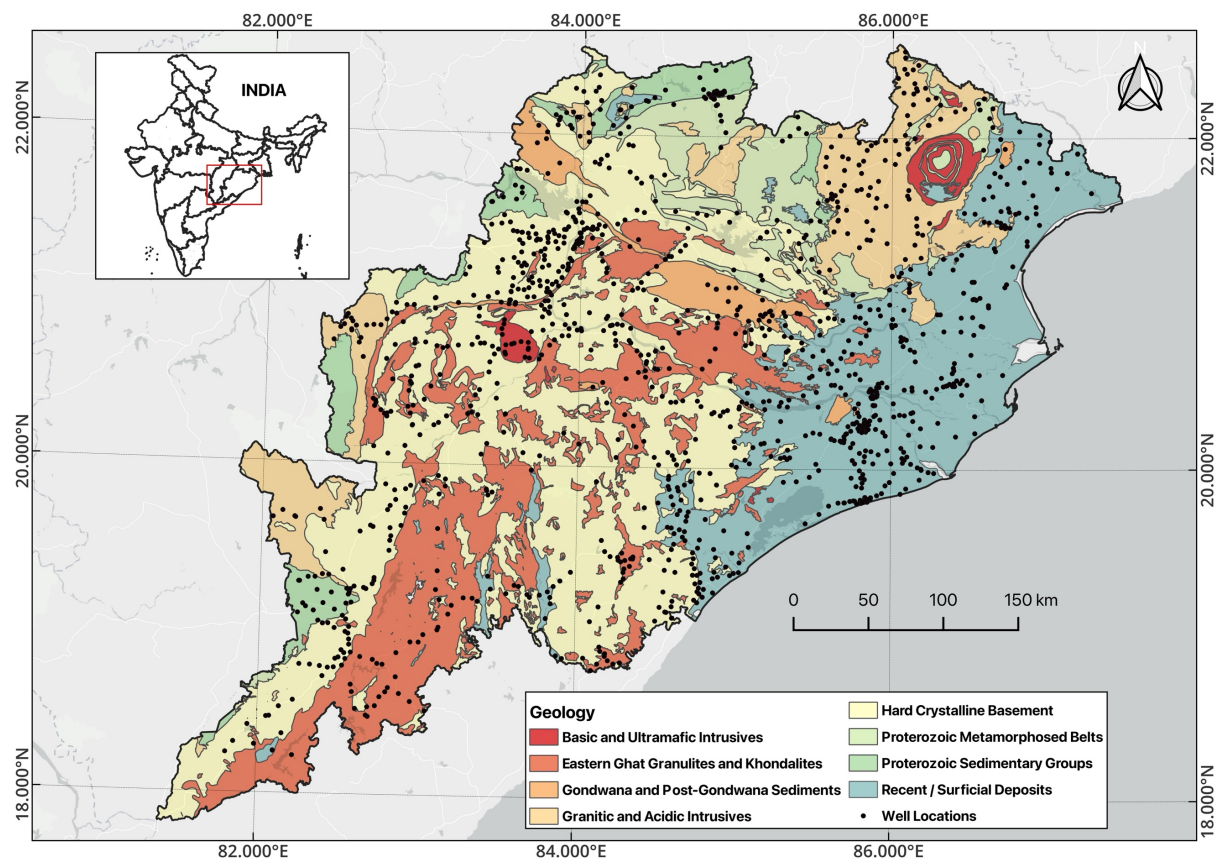


Figure 1. Location of the study area

2.2 Data Collection and Preprocessing

This study utilizes secondary groundwater quality data acquired from the Central Ground Water Board (([Dai et al., 2025](#); [Srivastava et al., 2024](#))) for the state of Odisha, covering the period from 2019 to 2023. The dataset comprises observations from 1280 monitoring locations. These sites capture the spatial heterogeneity of Odisha's aquifer systems, including coastal plains, hard rock uplands, and plateau regions.

Each monitoring location typically reports annual measurements for multiple hydrogeochemical parameters. To ensure temporal consistency and spatial comparability, the mean value for each parameter was calculated across the five-year period. When all five yearly records were available for a location, the average was computed using the complete set. In cases where only partial data existed, the mean was derived using the available values. For locations with only a single recorded value for a given parameter, that value was retained without modification. This aggregation approach ensured completeness of the dataset while preserving the representative hydro chemical characteristics of each location.

Thirteen groundwater quality parameters were initially selected based on their relevance to drinking water standards and their geochemical significance. These included pH, electrical conductivity (EC), total dissolved solids (TDS), bicarbonate (HCO_3^-), chloride (Cl^-), sulphate (SO_4^{2-}), nitrate (NO_3^-), total hardness (TH), calcium (Ca^{2+}), magnesium (Mg^{2+}), sodium (Na^+), potassium (K^+), and fluoride (F^-). The resulting temporally aggregated dataset served as the foundation for all subsequent correlation analysis, entropy-based modelling, and spatial interpretation.

2.3 Variable Selection and Multicollinearity Assessment

To ensure the stability of the proposed quantum entropy-based modelling framework and to avoid redundancy among input parameters, correlation and multicollinearity diagnostics were carried out. Pearson correlation analysis was first performed to examine the strength of linear relationships among the thirteen groundwater quality parameters. This helped in identifying highly correlated pairs that may introduce redundancy in weight computation and influence index sensitivity.

To further assess multicollinearity, the Variance Inflation Factor (VIF) was calculated for each parameter (O'brien, 2007). A commonly accepted threshold of VIF greater than 10 was used to indicate severe multicollinearity. Based on this criterion, four parameters exhibiting strong multicollinearity with others were excluded from further analysis. The refined dataset retained nine parameters for entropy-based weight generation and QEGWI formulation. These included pH, EC, SO_4^{2-} , NO_3^- , Ca^{2+} , Mg^{2+} , Na^+ , K^+ , and F^- .

No statistical outlier removal was applied to the dataset. This decision was based on the understanding that extreme values in groundwater datasets often reflect real geochemical processes or anthropogenic contamination events rather than measurement errors. Retaining these values allows for a more realistic estimation of parameter variability and improves the sensitivity of entropy-based weighting, especially in identifying zones with potential groundwater quality risks (Uddin et al., 2024).

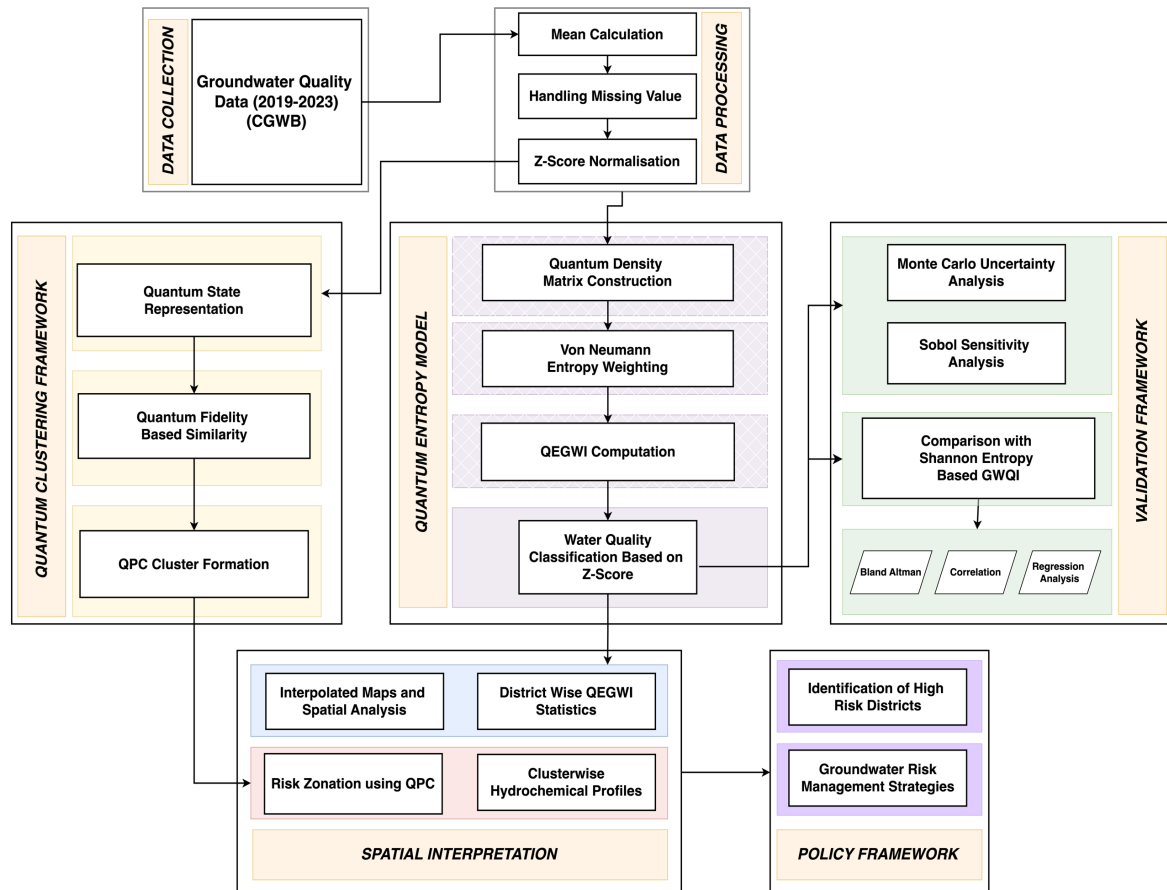


Figure 2. Methodological workflow outlining the QEGWI and QPC for spatial risk mapping

2.4 Descriptive Statistics and Hydro chemical Exploration

Descriptive statistical analysis was conducted to understand the central tendency and dispersion characteristics of the selected groundwater quality parameters. For each of the nine retained parameters, basic statistical measures including mean, standard deviation, minimum, maximum, coefficient of variation, Skewness and Kurtosis were computed. This helped to quantify the extent of variability across sampling locations and provided preliminary insights into the geochemical behaviour of each parameter. The observed variability also supported the

justification for using entropy-based weighting, as parameters with higher uncertainty are expected to carry more influence within the index formulation.

In addition to numerical summaries, Piper trilinear plot was constructed to classify water types and assess the relative dominance of major cations and anions across the dataset (Piper, 1944). These visual tools offered an initial indication of ionic balance, aquifer conditions, and spatial hydro chemical trends, which were later validated through entropy-based assessments and spatial analysis.

2.5 Theoretical framework

The QEGWI framework employs the density matrix formulation from quantum mechanics to represent the groundwater system as a probabilistic ensemble of normalized state vectors. Each state vector encapsulates a hydrogeochemical parameter and its spatial behaviour, while the resulting density matrix captures the full multivariate dependency structure across parameters (Nielsen & Chuang, 2010). This representation allows the use of von Neumann entropy, a generalization of Shannon entropy, to measure uncertainty within the system by accounting for both individual parameter variance and mutual information (Neumann, 1955). The entropy value of each parameter is then inverted and normalized to derive its weight, ensuring that more stable and informative parameters exert greater influence on the final QEGWI score. This weighting framework resolves a key limitation of classical entropy-based indices by dynamically adapting to spatial and inter-parameter variability.

The second methodological innovation, Quantum Probabilistic Clustering (QPC), extends these principles to soft classification of groundwater quality regimes. Each monitoring location is treated as a quantum state in a Hilbert space, constructed as a linear combination of orthonormal basis vectors corresponding to hydrogeochemical parameters (Dirac, 1981) state is encoded as a site-specific density matrix, capturing localized multivariate behaviour. Pairwise similarity between sites is measured using quantum fidelity, a metric that quantifies the closeness of two quantum states by comparing their density matrices (Jozsa, 1994). This fidelity measure replaces conventional Euclidean distances, allowing for a more nuanced probabilistic assessment that can tolerate overlap and transitions between regimes. Cluster assignment is achieved via projection operators that define soft boundaries, followed by optimization using a Quantum Expectation-Maximization (QEM) algorithm (Aïmeur et al., 2013). The QEM procedure iteratively updates cluster centroids and membership probabilities, converging to a stable probabilistic partition that inherently reflects uncertainty.

Quantum entropy, as applied in this study, serves as a statistical measure of multidimensional uncertainty rather than a physical property of quantum systems. Specifically, the von Neumann entropy captures the probabilistic structure and interdependence among hydrogeochemical parameters by encoding them in a density matrix. This approach extends classical entropy by accounting for parameter correlations and overlapping variances, making it well-suited for analysing groundwater quality under spatial heterogeneity and uncertainty.

The whole methodological framework of the study has been explained using the flowchart (fig. 2)

2.6 QEGWI Computation and Formulation

The Quantum Entropy Groundwater Quality Index (QEGWI) was developed to integrate uncertainty-aware parameter weighting with standardized groundwater quality data. The formulation involves six sequential steps as outlined below.

Step 1: Z-score Normalization

To ensure comparability across parameters and minimize sensitivity to extreme values, Z - score normalization was applied to the raw groundwater quality data:

$$Z_{ij} = \frac{X_{ij} - \mu_i}{\sigma_i} \quad (1)$$

where Z_{ij} is the standardized value of parameter f at site j , X_{ij} is the original concentration, μ_i is the mean, and σ_i is the standard deviation of parameter i .

Step 2: Construction of the Quantum Density Matrix

The quantum density matrix ρ is used to represent the multivariate probabilistic state of the hydrogeochemical system. It is formulated as:

$$\rho = \sum_{i=1}^m p_i |\psi_i\rangle \langle \psi_i| \quad (2)$$

Here, p_i denotes the probability weight associated with parameter i , and $|\psi_i\rangle$ is the normalized state vector of the parameter. The density matrix captures both the variability and interdependence among parameters in the standardized data.

Step 3: Computation of Quantum Entropy

The entropy of the system is computed using the von Neumann entropy formula:

$$S(\rho) = - \sum_{i=1}^n p_i \log p_i \quad (3)$$

This entropy measure quantifies the uncertainty or disorder in the groundwater quality system. Higher entropy implies more randomness and lower informational contribution from that parameter.

Step 4: Derivation of Quantum Entropy Weights

To convert entropy values into parameter weights, the following transformation is used:

$$W_i = \frac{1 - S_i}{\sum_{i=1}^n (1 - S_i)} \quad (4)$$

where W_i is the weight of parameter i , and S_i is its entropy value. Parameters with lower entropy (more informative and consistent) receive higher weights.

Step 5: Computation of QEGWI

The final index value for each location j is computed as a weighted inner aggregation of standardized parameter scores:

$$QEGWI_j = \sum_{i=1}^n W_i \cdot Z_{ij} \quad (5)$$

where Z_{ij} is the Z-score of parameters i at site j , and W_i is the quantum entropy-based weight.

Step 6: Classification of Groundwater Quality

QEGWI values were classified into five qualitative categories using standard deviation-based thresholds (*Table 1*). This classification helps interpret groundwater quality relative to the mean performance across the state:

Table.1. Classification scheme for QEGWI

QEGWI Range	Water Quality Category	Interpretation
≥ 1.5	Highly Unsafe	Severe contamination, unsuitable
$0.5 \text{ to } < 1.5$	Unsafe	Not suitable for consumption
$-0.5 \text{ to } < 0.5$	Moderate	Acceptable with treatment
$-1.5 \text{ to } < -0.5$	Safe	Suitable for drinking
< -1.5	Very Safe	Excellent quality

These thresholds are based on standard deviations from the mean QEGWI scores, allowing relative classification of groundwater quality across sites in the study area.

2.7 Quantum Probabilistic Clustering for Risk Zone Identification

Step 1: Quantum State Representation of Groundwater Sites

Each groundwater monitoring site is represented as a quantum state vector in an m -dimensional Hilbert space, where m is the number of hydrogeochemical parameters. The quantum state of the i^{th} site is given by:

$$|\psi_i\rangle = \sum_{j=1}^m p_{ij} |j\rangle \quad (6)$$

Here, p_{ij} is the probability amplitude associated with parameter j at site i , and $|j\rangle$ is the orthonormal basis vector corresponding to the j^{th} parameter. The state vector is normalized such that:

$$\sum_{j=1}^m |p_{ij}|^2 = 1 \quad \forall i \quad (7)$$

Step 2: Quantum Density Matrix Construction

To encode the probabilistic distribution and correlations within the groundwater system, a density matrix ρ_i is constructed for each site:

$$\rho_i = |\psi_i\rangle\langle\psi_i| \quad (8)$$

The overall ensemble density matrix capturing the entire system is given as a weighted mixture:

$$\rho = \sum_{i=1}^n w_i \rho_i = \sum_{i=1}^n w_i |\psi_i\rangle\langle\psi_i| \quad (9)$$

where w_i is the relative importance or weight of site i , typically taken as uniform unless external weights are provided.

Step 3: Quantum Fidelity as a Similarity Measure

To measure similarity between any two groundwater sites i and j , quantum fidelity is used:

$$F(\rho_i, \rho_j) = \left(\text{Tr} \left[\sqrt{\sqrt{\rho_i} \rho_j \sqrt{\rho_i}} \right] \right)^2 \quad (10)$$

Fidelity ranges from 0 (completely dissimilar) to 1 (identical states), allowing for a robust probabilistic similarity measure between spatially distributed water quality states.

Step 4: Probabilistic Cluster Membership via Projection Operators

Each cluster k is represented by a projection operator Π_k . The probability of a site i belonging to cluster k is computed as:

$$P(i \in k) = \frac{\text{Tr}(\rho_i \Pi_k)}{\sum_{j=1}^K \text{Tr}(\rho_i \Pi_j)} \quad (11)$$

where K is the total number of clusters. This soft assignment enables overlapping clusters, capturing uncertainty in transition zones.

Step 5: Quantum Expectation-Maximization (QEM) Algorithm

Cluster centroids (i.e., quantum prototypes) are iteratively updated using the QEM framework:

E-step: Calculate cluster membership probabilities $P(i \in k)$ using quantum fidelity.

M-step: Update the centroid density matrix for each cluster:

$$\rho_k^{(t+1)} = \frac{1}{N_k} \sum_{i=1}^N P(i \in k) \rho_i \quad (12)$$

where $\rho_k^{(t+1)}$ is the updated centroid for cluster k , and $N_k = \sum_{i=1}^N P(i \in k)$ is the effective cluster size. The algorithm iterates until convergence is achieved based on stability of cluster assignments or a defined maximum iteration threshold.

Step 6: Spatial Mapping and Risk Zone Classification

The resulting probabilistic clusters are spatially interpolated using geostatistical techniques to generate continuous cluster probability surfaces. Each location is then classified into groundwater risk zones (high, medium, or low) based on the dominant cluster membership and its confidence level.

To quantify uncertainty, cluster entropy is computed at each site:

$$H_i = - \sum_{k=1}^K P(i \in k) \log P(i \in k) \quad (13)$$

High entropy indicates uncertainty in cluster assignment and highlights regions that may require further investigation or additional sampling.

2.8 Model Validation and Sensitivity Analysis

To ensure the robustness, reliability, and scientific validity of the proposed Quantum Entropy-based Groundwater Quality Index (QEGWI), a comprehensive model evaluation was conducted. This included sensitivity analysis, uncertainty quantification, and comparative performance benchmarking against the established Shannon Entropy-based GWQI (SE-GWQI).

2.8.1 Sobol Sensitivity Analysis

Global sensitivity analysis was performed using the Sobol method to assess the relative influence of each hydrogeochemical parameter on the QEGWI (Sobol, 2001). This variance-based approach decomposes the total output variance into contributions from individual parameters and their higher-order interactions.

Let $Y = f(X_1, X_2, \dots, X_n)$ represent the QEGWI as a function of input parameters. The Sobol firstorder sensitivity index S_i is given by:

$$S_i = \frac{\text{Var}_{X_i} [E_{X_{\sim i}}(Y | X_i)]}{\text{Var}(Y)} \quad (14)$$

and the total-order sensitivity index S_{Ti} is:

$$S_{Ti} = \frac{E_{X_{\sim i}} [\text{Var}_{X_i} (Y | X_{\sim i})]}{\text{Var}(Y)} \quad (15)$$

Parameters with high S_i and S_{Ti} values were found to significantly influence QEGWI scores, thereby guiding parameter prioritization in water quality monitoring.

2.8.2 Monte Carlo Uncertainty Analysis

To evaluate the propagation of uncertainty through the QEGWI framework, a Monte Carlo simulation was performed (Helton & Davis, 2003). Each hydrogeochemical parameter was sampled from its empirical distribution across 10,000 iterations. QEGWI scores were computed in each iteration to generate a distribution of index values per site.

From this, the uncertainty bounds and confidence intervals of QEGWI were derived, enabling the identification of sites with high output uncertainty due to parameter variability. The simulation also confirmed the model's stability across diverse sampling scenarios, reinforcing its suitability for policy oriented applications.

2.8.3 Comparative Evaluation with Shannon Entropy-based GWQI

To ensure a rigorous benchmarking of the proposed Quantum Entropy-based Groundwater Quality Index (QEGWI), a parallel index was formulated using Shannon entropy-based weighting, referred to as SE-GWQI. This comparative assessment was not intended to promote SE-GWQI as a standalone method but to validate the stability, interpretability, and performance of QEGWI. Four levels of evaluation were employed: (i) correlation analysis using both Pearson's and Spearman's coefficients to assess overall consistency between the indices; (ii) Bland–Altman agreement analysis to examine systematic bias and limits of agreement (Giavarina, 2015); (iii) regression modelling supported by LOWESS smoothing to evaluate linearity and potential non-linear deviations across contamination gradients; and (iv) categorical agreement analysis using a confusion matrix based on a five-class groundwater quality scheme.

2.8.4 Silhouette analysis

To evaluate the internal consistency of the Quantum Probabilistic Clustering (QPC) framework, silhouette analysis was conducted using the fidelity-derived distance matrix (Rousseeuw, 1987). The silhouette score quantifies how well each data point fits within its

assigned cluster compared to other clusters, with values ranging from -1 to $+1$. A higher silhouette score indicates greater cohesion within clusters and better separation between them. Given the soft probabilistic nature of QPC, this validation provides a meaningful measure of clustering quality, especially in transitional zones where conventional hard clustering metrics fall short. The analysis employed a precomputed distance matrix derived from quantum fidelity, ensuring compatibility with the probabilistic geometry of the Hilbert space.

3. RESULTS

3.1 Hydrogeochemical Characteristics

K^+ exhibited the highest coefficient of variation (171.07%), followed by Na^+ (118.52%) and NO_3^- (115.48%), indicating strong dispersion and the presence of outliers. In contrast, pH showed minimal variability ($CV = 4.07\%$), while TH displayed moderate variation ($CV = 52.47\%$). EC ranged from 63 to 8808.33 $\mu S/cm$, TDS from 43.5 to 2911 mg/L, F^- from 0 to 4.145 mg/L, and NO_3^- from 0 to 267.75 mg/L. EC, Cl^- , SO_4^{2-} , NO_3^- , Na^+ , K^+ , and F^- were strongly right-skewed, reflecting anthropogenic or lithological influences, whereas pH had a mildly left-skewed distribution (-0.739). Kurtosis exceeded 50 for EC, Na^+ , K^+ , and SO_4^{2-} , indicating sharp peaks; pH remained near-normal (kurtosis = 4.35) (Table 2).

Table.2. Descriptive statistics of hydrogeochemical parameters

Parameters	Mean	SD	Min	Max	CV (%)	Skewness	Kurtosis
pH	7.864	0.32	5.32	9.09	4.067	0.739	4.348
EC	704.665	567.101	63	8808.333	80.478	5.754	60.425
TDS	377.701	269.479	43.5	2911	71.347	2.686	13.45
HCO_3^3	216.875	111.079	10	910	51.218	1.231	3.86
Cl^-	82.303	94.339	1	1456	114.624	5.452	53.487
SO_4^{2-}	31.47	33.047	0	596	105.011	6.027	79.221
NO_3^-	19.564	22.592	0	267.75	115.477	4.598	38.251
TH	211.299	110.864	20	816	52.468	1.214	2.649
Ca	45.357	22.577	4	192.2	49.775	1.377	4.162
Mg	24.172	16.576	1	154.46	68.576	1.658	5.19
Na^+	51.959	61.582	1	945	118.518	5.937	58.899
K^+	12.647	21.635	0	367.5	171.073	6.057	67.828
F^-	0.403	0.356	0	4.145	88.52	2.818	14.73

pH values cluster near neutral to slightly alkaline levels, remaining within acceptable limits. EC and TDS mostly fall below 1000 $\mu S/cm$ and 1000 mg/L, respectively, though long right-skewed tails mark isolated zones of elevated salinity beyond WHO (2017) thresholds. HCO_3^-

is concentrated between 100–400 mg/L, while Cl^- and SO_4^{2-} show broader spreads with exceedances of guideline values. NO_3^- is positively skewed, with most samples below 45 mg/L but some exceeding 200 mg/L, suggesting localized contamination. TH, Ca^{2+} , and Mg^{2+} exhibit extended upper tails, consistent with hardness variability. Na^+ and K^+ are highly skewed, with K^+ showing extreme outliers. F^- concentrations surpass 1.5 mg/L in select areas, indicating potential fluoride-related health risks (fig 3a).

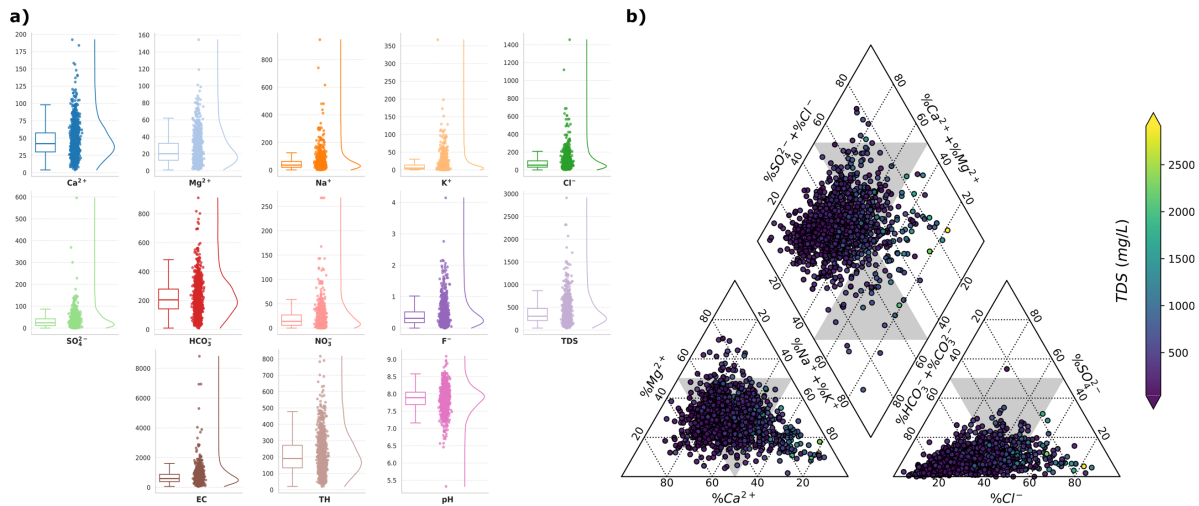


Figure 3 Hydrogeochemical characterization of groundwater samples **a)** Raincloud plots **b)** Piper trilinear diagram

The trilinear Piper diagram revealed distinct hydro chemical facies across Odisha (fig. 3b). In the cation triangle, groundwater samples predominantly clustered near the Ca^{2+} and Mg^{2+} apexes, indicating dominance of alkaline earth metals, with $\text{Na}^+ + \text{K}^+$ contributing minimally. The anion triangle showed a strong presence of Cl^- and SO_4^{2-} , with moderate representation from $\text{HCO}_3^- + \text{CO}_3^{2-}$. In the central diamond field, most samples plotted within the mixed Ca^{2+} – Mg^{2+} – Cl^- and Ca^{2+} – Mg^{2+} – SO_4^{2-} facies, suggesting mixed water types. The TDS colour gradient highlighted that the majority of samples had values below 1000 mg/L, though a few exceeded 2000 mg/L, indicating localized salinity hotspots.

Spatial distribution Cl^- and SO_4^{2-} concentrations peak in southern and southeastern Odisha, while NO_3^- shows isolated hotspots in northern and eastern zones, indicating possible anthropogenic inputs. F^- levels exceed WHO limits in parts of western and central districts, aligning with fluoride-bearing lithologies. HCO_3^- dominates in central and western regions due to carbonate weathering. Among cations, Ca^{2+} and Mg^{2+} show elevated levels in the hard-rock regions of western Odisha, reflecting strong rock–water interactions. Na^+ and K^+ exhibit scattered enrichments— Na^+ concentrations rise near coastal belts, while K^+ hotspots suggest localized agricultural sources. EC and TDS display steep spatial gradients, with high values in

coastal and central zones, indicating salinity ingress and poor flushing. TH mirrors the spatial pattern of Ca^{2+} and Mg^{2+} , while pH remains uniformly alkaline across districts (fig 4).

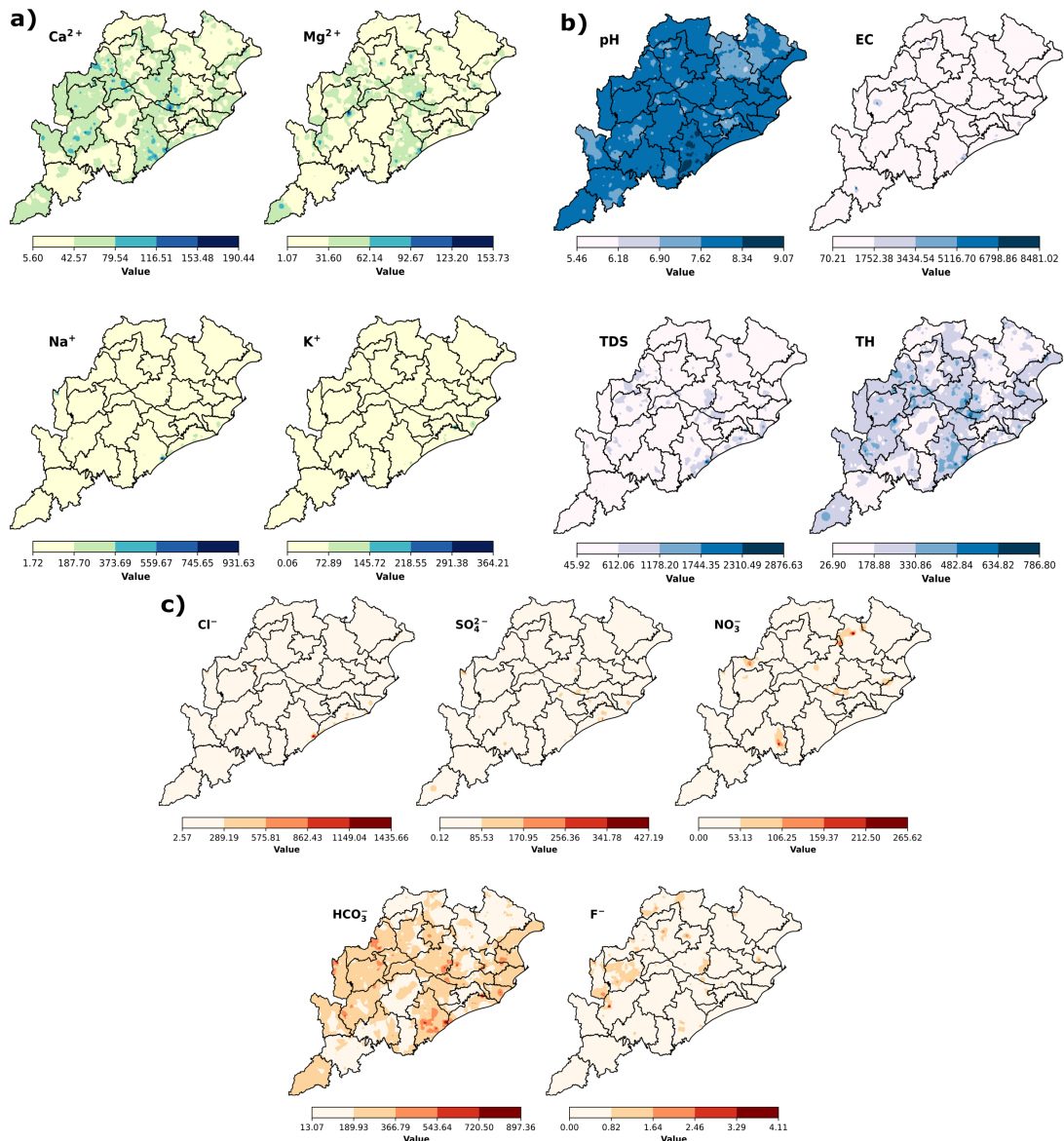


Figure 4 Spatial distribution of groundwater quality parameters across the study region a) Cations b) General water quality parameters c) Anions

3.2 Quantum Entropy Groundwater Quality Index (QEGWI)

The spatial distribution of QEGWI classifications across Odisha reveals considerable heterogeneity in groundwater quality risk, with several districts exhibiting alarming proportions of unsafe conditions (Fig. 6). Notably, Anugul recorded the highest proportion of Unsafe sites (40.0%) and a substantial presence of Highly Unsafe zones (6.0%). Similar trends were observed in Puri (36.0% Unsafe, 8.0% Highly Unsafe), Ganjam (28.7% Unsafe, 3.4% Highly Unsafe), and Balangir (25.8% Unsafe, 1.6% Highly Unsafe), indicating pronounced

vulnerability in these districts. Bhadrak, despite a relatively lower proportion of Unsafe sites, recorded the highest share of Highly Unsafe classifications (10.5%), emphasizing localized groundwater contamination hotspots. Several districts showed strong dominance of the Moderate category, reflecting borderline water quality that may become unsafe under changing hydrogeochemical or anthropogenic stress. Malkangiri stood out with 91.7% of its groundwater sites falling under the Moderate class, followed closely by Nuapadha (88.0%), Baudh (80.0%), and Nabarangapur, Kendrapara, Jagatsinghpur, Baragarh, Balangir, Sambalpur, and Cuttack—each exceeding 70% Moderate representation. On the other end, Koraput emerged as the safest district, with 67.2% of sites classified as Safe and no observations in the Unsafe or Highly Unsafe categories. Other relatively safer districts included Kandhamal (52.9% Safe), Kendujhar (45.5%), Khordha (43.8%), and Mayurbhanj (43.2%), suggesting stable hydrogeochemical conditions and limited contamination risk (fig. 5). These point-based risk patterns are spatially mirrored in the interpolated QEGWI surfaces, where high mean values and standard deviations reinforce district-level vulnerability identified through categorical classification.

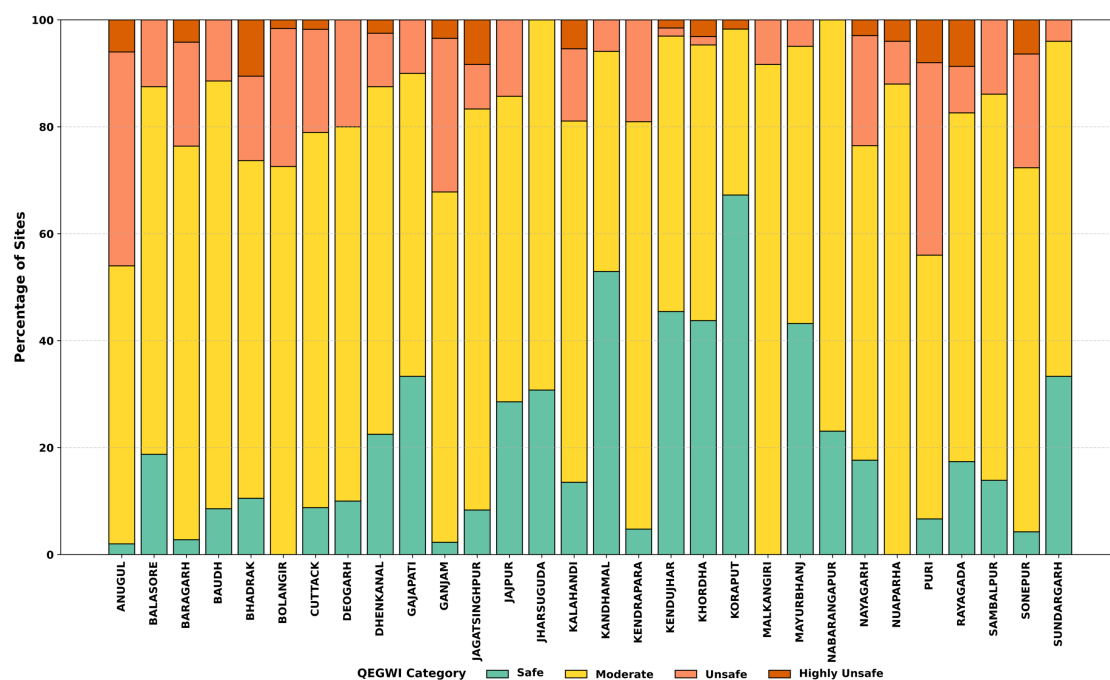


Figure 5 District-wise distribution of groundwater quality categories based on QEGWI

District-level raster statistics indicate that Angul exhibited the highest mean QEGWI (0.24), with peak values exceeding 2.15. Bargarh (mean = 0.21, max > 1.75, SD = 0.40) and Bolangir (mean = 0.22, SD = 0.28) also recorded elevated values, suggesting widespread but spatially consistent groundwater quality degradation. In contrast, coastal districts such as Balasore (mean = -0.04, min = -0.87) and Bhadrak (mean = 0.13) reported lower mean scores, though

localized hotspots still breached the 1.75 threshold. The overall distribution of QEGWI across districts are characterized by high standard deviations in several regions.

A substantial 77.41% of the total area (~120,586 km²) falls under the Moderate category, suggesting widespread borderline water quality. Only 13.73% (~21,393 km²) of the area is classified as Safe, while regions categorized as Unsafe and Highly Unsafe occupy 8.41% (~13,094 km²) and 0.46% (~710 km²), respectively (Table 3).

Table 3 district wise statistics of QEGWI

District	Mean	Min	Max	SD
Angul	0.24	0.66	2.15	0.42
Bolangir	0.22	0.47	1.75	0.28
Balasore	0.04	0.87	1.06	0.26
Bargarh	0.21	0.74	2.29	0.40
Bhadrak	0.13	0.64	1.79	0.38
Cuttack	0.16	1.25	2.01	0.49
Deogarh	0.02	0.59	0.88	0.25
Dhenkanal	0.10	0.80	1.66	0.37
Gajapati	0.37	1.02	0.91	0.30
Ganjam	0.33	0.69	4.37	0.46
Jagatsinghpur	0.25	0.64	2.31	0.57
Jajpur	0.06	0.76	0.98	0.38
Jharsuguda	0.29	0.74	0.86	0.16
Kalahandi	0.02	0.65	2.39	0.37
Kandhamal	0.33	0.81	0.85	0.23
Kendrapara	0.09	0.64	1.18	0.22
Kendujhar	0.35	1.02	2.31	0.34
Khordha	0.19	0.96	3.78	0.52
Koraput	0.55	0.95	1.64	0.20
Malkangiri	0.06	0.65	1.07	0.29
Mayurbhanj	0.41	0.92	1.02	0.26
Nabarangapur	0.11	0.80	0.81	0.21
Nayagarh	0.09	0.86	1.58	0.35
Nuaparha	0.28	0.42	4.99	0.43
Puri	0.34	0.89	5.26	0.53
Rayagada	0.11	0.86	2.31	0.37
Sambalpur	0.16	0.87	1.45	0.27
Sonepur	0.20	0.57	2.22	0.32
Sundargarh	0.22	0.92	1.38	0.23
Baudh	0.06	1.00	0.91	0.27

Districts like Angul, Puri, Ganjam, and Balangir consistently emerge as critical zones. From the point-based statistics, these districts record the highest proportion of sites in the Unsafe and Highly Unsafe categories (e.g., Angul: 40% Unsafe, 6% Highly Unsafe; Puri: 36%, 8%). The interpolated raster analysis reinforces this trend, with Angul displaying the highest mean QEGWI (0.24) and extreme maximum values (>2.15), signifying persistent and widespread contamination risks. Similarly, Balangir and Bargarh exhibit high mean values (>0.20) in raster analysis and elevated unsafe proportions at the point level, indicating both spatial continuity and point-specific risk hotspots. In contrast, districts like Koraput, Kandhamal, and Mayurbhanj are identified as safer zones in both assessments. Koraput, in particular, shows 67.2% of sites as Safe with no unsafe records, aligning with consistently low raster QEGWI values.

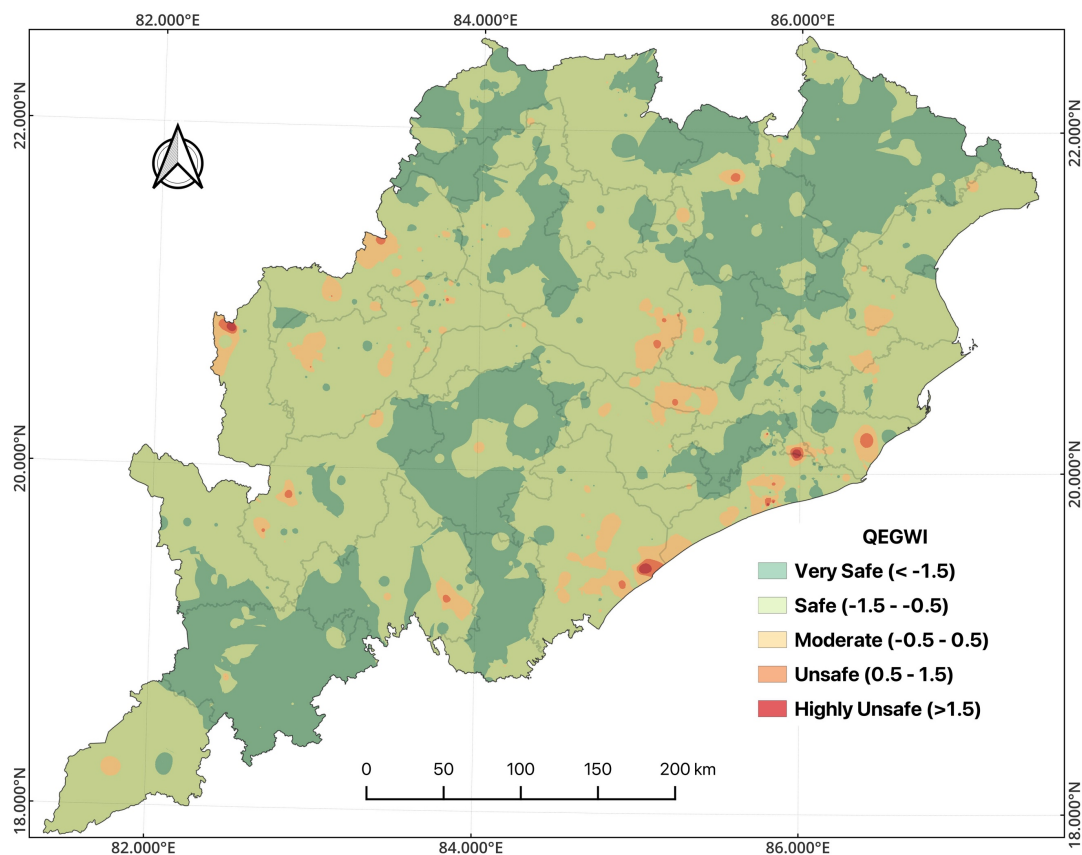


Figure 6 Spatial distribution of groundwater quality in Odisha based on the QEGWI).

3.3 QPC for Groundwater Regime Classification

To complement the spatially continuous QEGWI and introduce a robust classification mechanism capable of reflecting uncertainty and overlapping regimes, Quantum Probabilistic Clustering (QPC) was employed. This method represents each groundwater location as a

quantum state in a Hilbert space, using density matrices to encode hydro chemical variability and probabilistic similarity through fidelity measures.

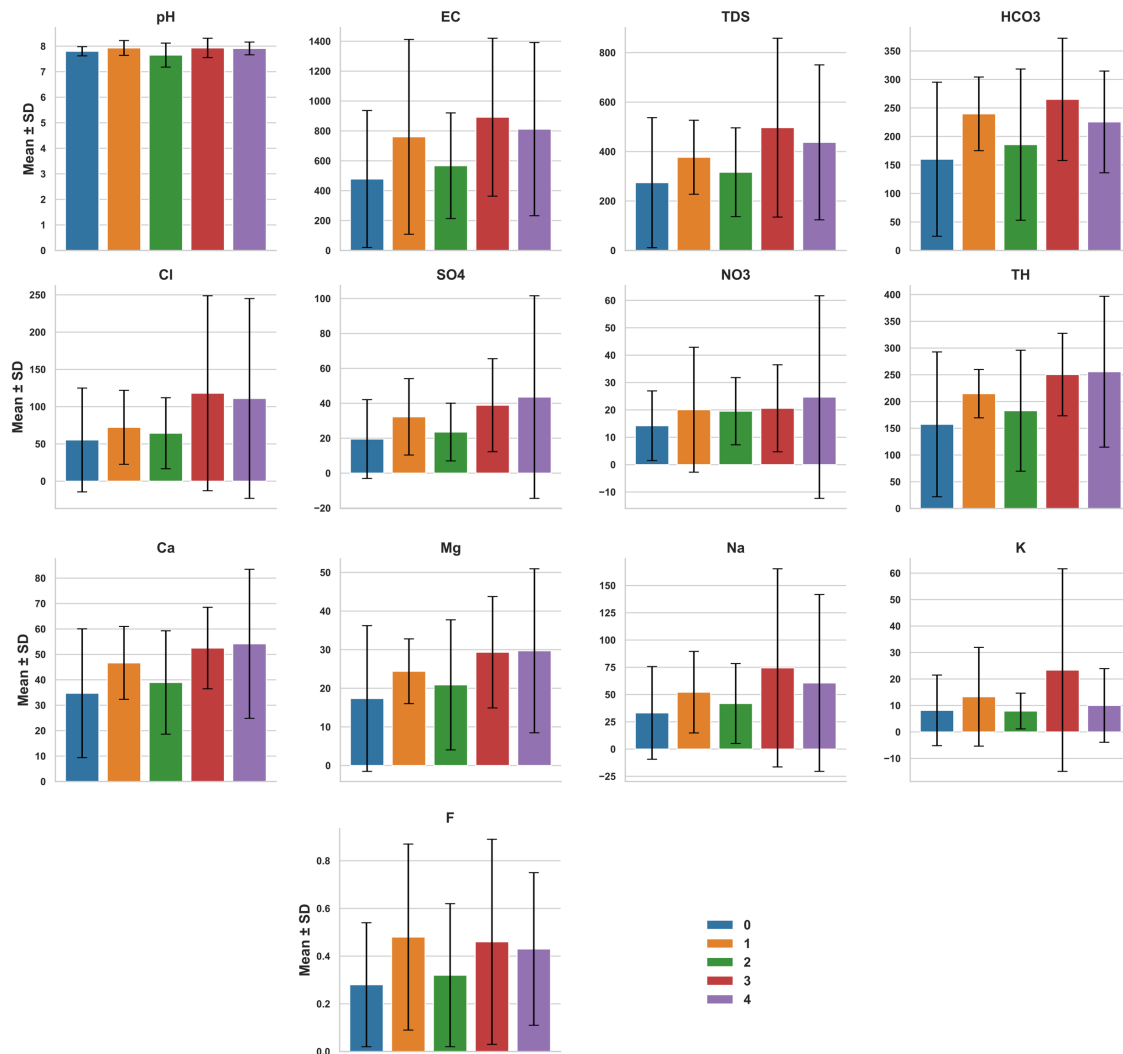


Figure 7 Cluster-wise mean and standard deviation of groundwater quality parameters across QPC groups

Clusters 3 and 4 emerged as the most contamination-prone segments, with both exhibiting elevated concentrations of salinity-indicative ions (EC, NO_3^- , F^-). Cluster 3 reported the highest electrical conductivity (EC: 891.69 $\mu\text{S}/\text{cm}$) and total dissolved solids (TDS: 496.64 mg/L), indicative of significant salinity and dissolved ion load. It also showed elevated Na^+ (74.47 mg/L) and K^+ (23.37 mg/L) concentrations, along with high levels of NO_3^- (20.59 mg/L) and F^- (0.46 mg/L), reflecting anthropogenic and geogenic contamination. Cluster 4, while slightly lower in EC (811.70 $\mu\text{S}/\text{cm}$) and TDS (437.11 mg/L), surpassed all clusters in NO_3^- concentration (24.69 mg/L) and exhibited the highest standard deviations in EC and Na^+ , pointing to sharp localised risk zones. Its spatial alignment with QEGWI hotspot districts such as Angul and Balangir substantiates its high-risk designation (fig. 7). Cluster 1 reflected moderate degradation with intermediate EC and TDS levels and the highest F^- concentration

(0.48 mg/L), suggesting early-stage water quality deterioration. Conversely, Clusters 0 and 2 recorded the lowest values across key contaminants (e.g., EC, TDS, NO_3^-), representing the chemically safest groups. This cluster-level hydro chemical differentiation reinforces the complementary role of QPC in validating and extending QEGWI-based spatial risk assessments.

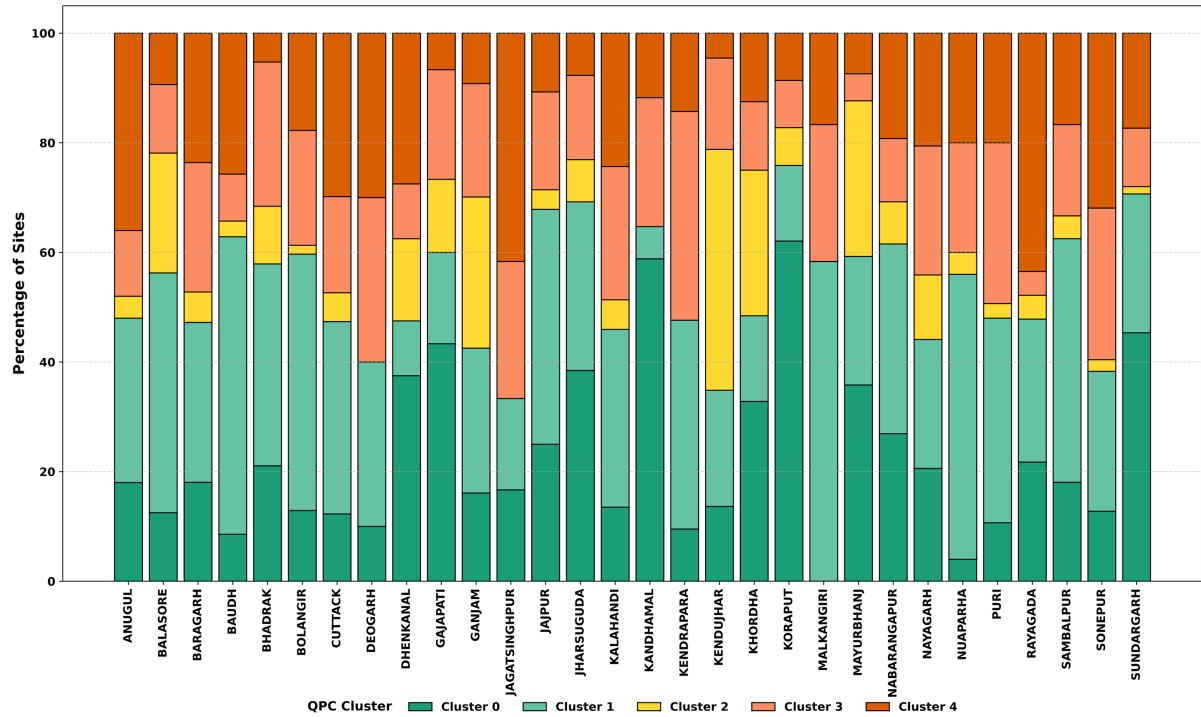


Figure 8. District-wise distribution of groundwater quality clusters derived from QP).

Spatial analysis of QPC outcomes further reinforced these distinctions, revealing structured patterns in groundwater vulnerability that aligned closely with QEGWI-derived risk zones (fig. 8). Cluster 4 was prominently distributed in critically stressed districts such as Anugul (35.6%), Puri (33.3%), Bhadrak (28.8%), and Ganjam (28.7%). These same districts recorded high Unsafe and Highly Unsafe proportions in the QEGWI analysis (e.g., Anugul and Puri exceeding 40%), thereby validating the hydro chemical risk profile of Cluster 4. Similarly, Cluster 3 showed elevated representation in Balangir (26.6%), Bhadrak (32.7%), and Baragarh (25.6%), which also had high mean QEGWI scores (>0.20) and frequent hotspot presence in both point-level and interpolated analyses. On the safer end of the spectrum, Cluster 0 was dominant in districts like Koraput (61.3%), Malkangiri (53.3%), and Nabarangapur (45.3%), all of which corresponded to predominantly Safe or Very Safe zones in QEGWI classification. Transitional districts such as Jagatsinghpur, Khordha, and Kendrapara showed mixed compositions of Clusters 1–3, reflecting their moderate QEGWI values and underlying spatial

heterogeneity (Fig 8). The spatial distribution of all the clusters across Odisha state has been shown in Fig 9.

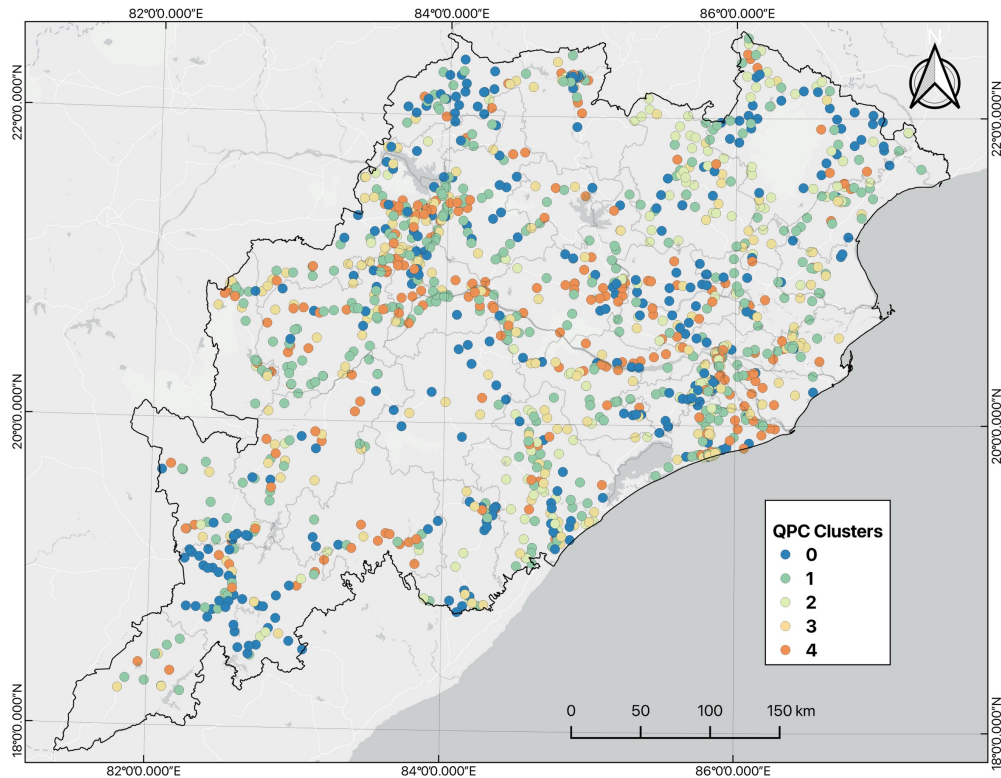


Figure 9 Spatial distribution of QPC of groundwater quality across Odisha.

3.4 Sensitivity Analysis

3.4.1 Sensitivity Analysis of QEGWI Parameters

Sensitivity analysis using Partial Correlation Coefficients (PCC) and Standardized Regression Coefficients (SRC) revealed distinct patterns in parameter influence on the QEGWI (Fig 10). EC emerged as the most dominant contributor (PCC = 0.82, SRC = 0.13), followed closely by Na^+ , SO_4^{2-} , and Mg^{2+} , each with high correlation and regression values (PCC > 0.75, SRC \approx 0.13). These parameters reflect both salinity and geogenic mineral dissolution processes and align with high entropy weights observed earlier in the study.

Ca^{2+} and K^+ showed moderate sensitivity; while Ca^{2+} had a relatively high PCC (0.67), its SRC (0.08) was comparatively lower, suggesting a more passive influence on QEGWI variability. In contrast, K^+ exhibited higher SRC (0.11) than its PCC (0.52), indicating a more conditional or model internal contribution. NO_3^- and F^- demonstrated lower sensitivities across both metrics (PCC \approx 0.44–0.47; SRC \approx 0.10), likely due to their spatially localized distribution rather than wide scale influence. pH consistently showed the lowest influence (PCC = 0.35,

SRC = 0.09), confirming its limited impact within the entropy based groundwater quality structure in this region.

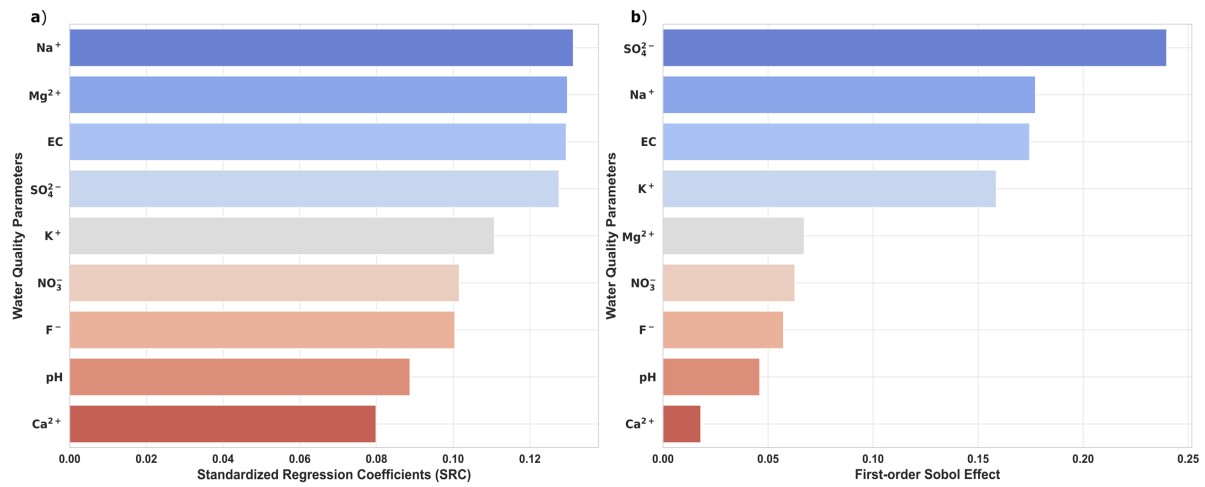


Figure 10 Global sensitivity analysis of groundwater quality parameters influencing QEGWI (a) Standardized Regression Coefficients (SRC) and (b) First-order Sobol indices

3.4.2 Global Sensitivity Analysis using Sobol Indices

The results revealed that SO₄²⁻ had the highest first order effect (0.240) and a total effect of 0.233, indicating a dominant and direct role in driving output variance. Na⁺ and EC followed closely, with first order effects of 0.177 and 0.175, respectively, and near identical total effects (0.179 and 0.175), reflecting their strong individual contributions with minimal interaction effects. K⁺ also exhibited a notable influence, with a first order index of 0.159, suggesting moderate sensitivity. In contrast, NO₃⁻, Mg²⁺, and F⁻ demonstrated lower but comparable sensitivities, with first order effects ranging between 0.057 and 0.067. pH and Ca²⁺ contributed the least to QEGWI variability, with pH having a first order effect of 0.046 and Ca²⁺ just 0.018. The narrow difference between first order and total effect indices across all parameters suggests that the QEGWI model structure is largely additive, with limited higher order interactions.

A standardized regression coefficient (SRC) (fig. 9) clearly ranks the influence of hydrogeochemical parameters on QEGWI. Na⁺, Mg²⁺, EC, and SO₄²⁻ emerge as the top contributors, each exhibiting SRC values exceeding 0.12, confirming their significant role in groundwater quality index variability. In contrast, Ca²⁺ and pH show minimal influence, further reinforcing their marginal contribution observed across other sensitivity metrics.

3.4.3 Uncertainty Analysis

Complementing the sensitivity plot, a Monte Carlo–derived uncertainty boxplot (fig. 12) displays the distribution of simulated parameter values, capturing their inherent variability under uncertainty propagation. NO_3^- , EC, Na^+ , and F^- exhibit broader interquartile ranges and a higher density of extreme values, indicative of localized fluctuations and spatial heterogeneity. In contrast, pH and Ca^{2+} demonstrate narrow distributions with low dispersion, validating their stability and limited impact on index variability.

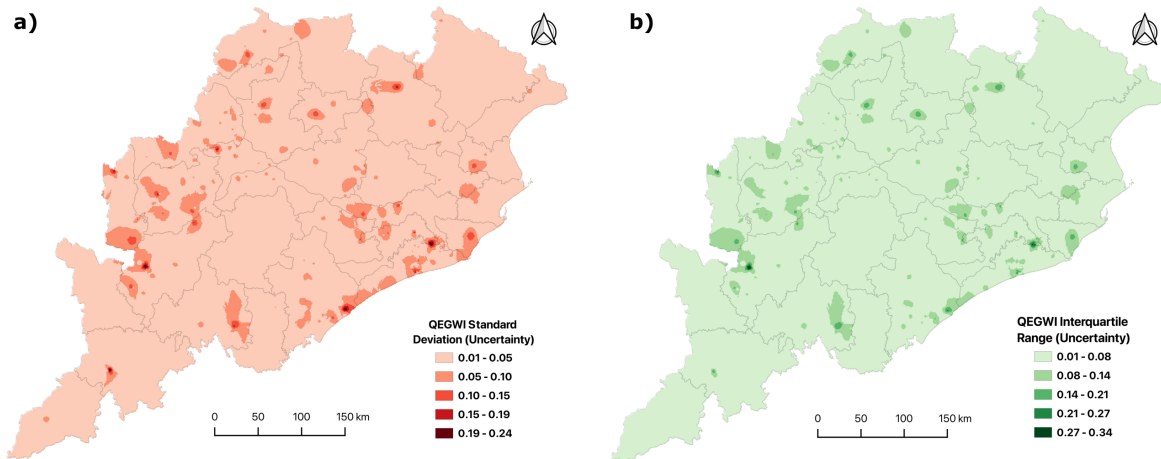


Figure 11 Uncertainty quantification in the QEGWI, (a) Spatial distribution of standard deviation (b) Spatial distribution of interquartile range

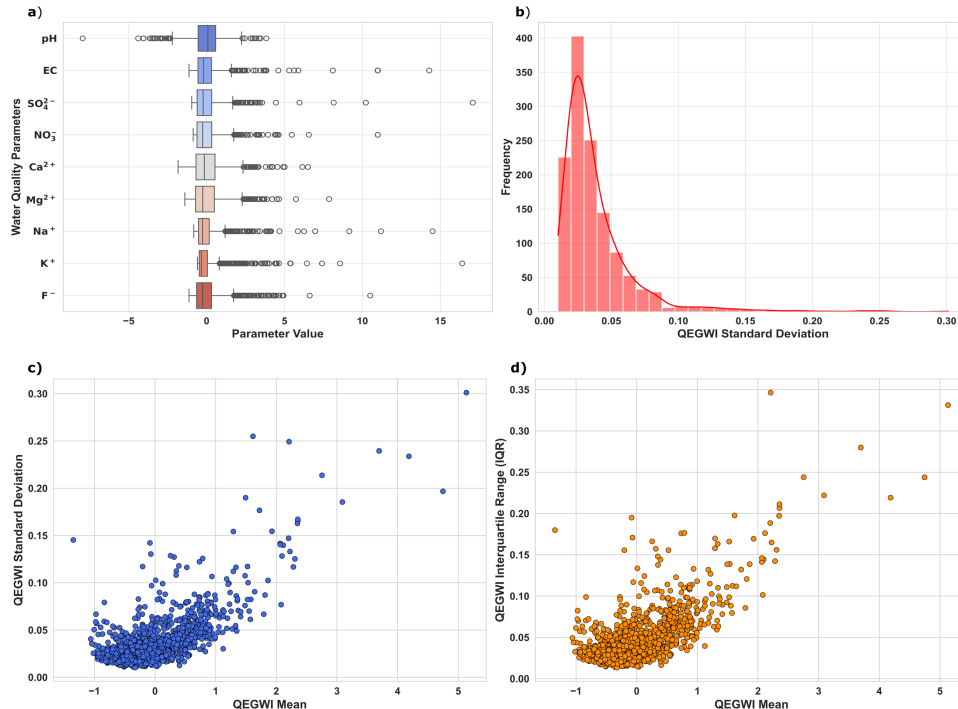


Figure 12 Uncertainty characterization and parameter variability in the QEGWI. (a) Boxplots showing the distribution of standardized values for key water quality parameters used in QEGWI computation (b) Histogram of QEGWI standard deviation with fitted distribution curve (c) Scatterplot of QEGWI mean vs. standard deviation (d) Scatterplot of QEGWI mean vs. interquartile range

To quantify the variability associated with the (QEGWI), a Monte Carlo–based uncertainty propagation analysis was performed, and the distribution of standard deviations and IQR across all spatial locations is presented in Figure 11. The histogram reveals a right skewed distribution, with the majority of QEGWI values exhibiting low standard deviation. Most locations recorded uncertainty below 0.05, indicating strong stability and robustness of the QEGWI formulation across the study area.

Only a small fraction of sites exhibited standard deviations greater than 0.10, and very few exceeded 0.20, suggesting that the influence of hydrogeochemical uncertainty on the final index is spatially constrained and does not pervasively affect index interpretation. The presence of a smooth kernel density curve overlay further confirms that uncertainty is heavily concentrated at the lower end of the distribution. This outcome supports the methodological reliability of the quantum entropy based weighting scheme and highlights its effectiveness in minimizing spatial uncertainty during groundwater quality assessment.

3.4.4 Comparison with Shannon Entropy based GWQ

The comparative evaluation of the QEGWI against the Shannon Entropy–based GWQI (SE GWQI) revealed a near perfect agreement between the two methodologies. The Pearson correlation coefficient was 0.9979, and the Spearman correlation stood at 0.9982, both with p values < 0.001 , confirming an extremely strong linear and monotonic relationship between the scores derived from both indices. This high correlation is further corroborated by the regression plot, where the R^2 value of 1.00 signifies almost complete overlap in predictions. The regression trend, validated using a LOWESS fit, showed no observable bias, confirming the statistical equivalence of the two indices across most of the sampled locations.

However, the Bland Altman analysis offered more nuanced insights into the differences (fig. 13). The mean difference between QEGWI and SE GWQI was virtually zero, and most observations fell within the 95% limits of agreement, indicating excellent consistency. Yet, slight deviations were noted in the mid to high QEGWI range, where QEGWI tended to produce marginally higher values than SE GWQI. This deviation likely stems from QEGWI's sensitivity to spatial heterogeneity and its probabilistic weighting mechanism based on quantum entropy. The confusion matrix analysis further supported this, with a dominant match in the moderate and safe classes, but notable shifts in the “Unsafe” and “Highly Unsafe” categories where QEGWI identified slightly more locations under high risk. These shifts reflect QEGWI's enhanced capability to detect local anomalies, making it more suitable for

uncertainty aware decision making in groundwater quality management, especially in geochemically complex regions .

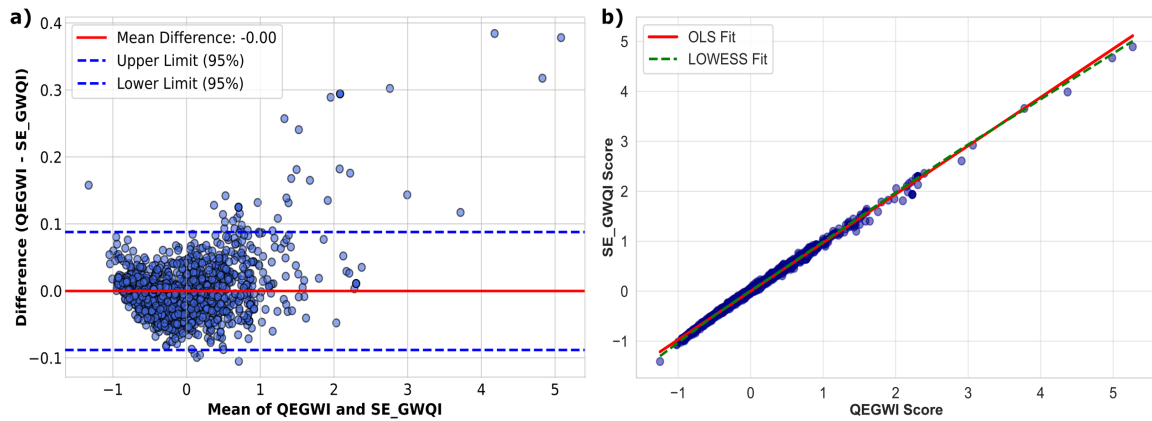


Figure 13 Validation of the QEGWI against the conventional Shannon Entropy-based GWQI (a) Bland–Altman plot comparing QEGWI and SE-GWQI scores (b) Scatterplot with OLS (Ordinary Least Squares) and LOWESS(Locally Weighted Scatterplot Smoothing)

3.4.5 Silhouette analysis

The silhouette analysis of the QPC yielded a mean silhouette score of 0.0588, indicating significant overlap among cluster boundaries. Unlike hard clustering methods that forcefully partition data into discrete, non-overlapping groups, QPC embraces the inherent ambiguity and fuzziness of hydrogeochemical systems by allowing samples to exhibit probabilistic associations across clusters.

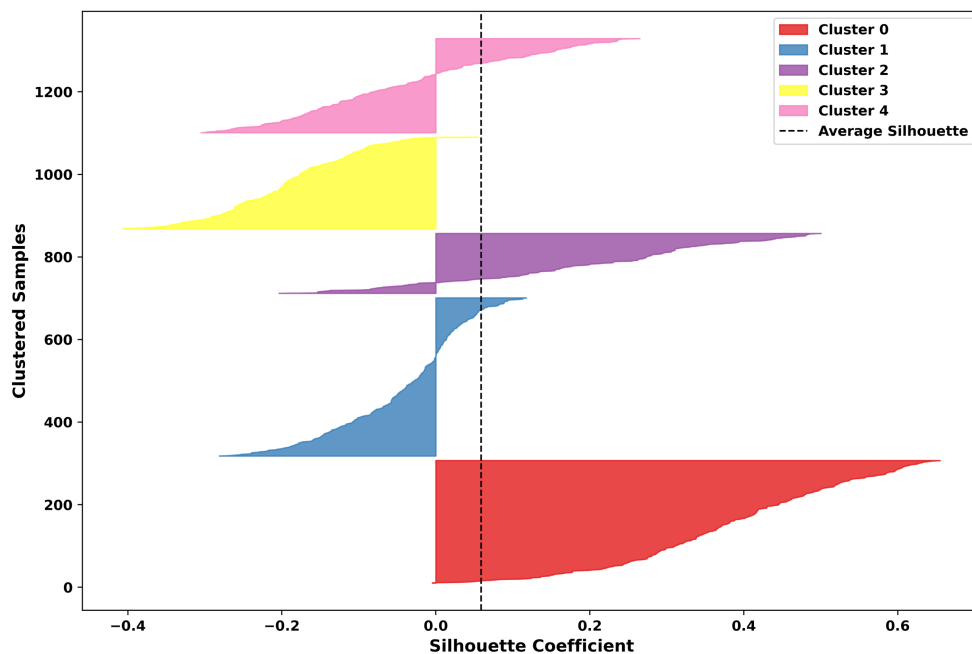


Figure 14 Silhouette analysis of Quantum Probabilistic Clustering (QPC) results

The silhouette plot (fig. 14) further reinforces this, showing substantial variation in silhouette coefficients within and across clusters, including negative values in clusters 1, 3, and 4. These

low or negative coefficients highlight the transitional nature of groundwater quality in Odisha, where samples do not cleanly separate into rigid clusters due to overlapping contaminant signatures and interacting geogenic and anthropogenic influences. The largest cluster (Cluster 0) displays the most cohesive structure with a wide distribution of positive silhouettes, while smaller clusters reveal mixed internal consistency.

4 DISCUSSION

The integration of the Quantum Entropy-based Groundwater Quality Index (QEGWI) and Quantum Probabilistic Clustering (QPC) in this study forms a cohesive, two-tiered framework that addresses both quantitative assessment and qualitative classification under uncertainty. While QEGWI offers a continuous, entropy-weighted risk score derived from multivariate hydrogeochemical uncertainty, QPC complements this by providing soft, probabilistic spatial delineation of groundwater quality regimes. The relationship is not merely sequential but synergistic: QEGWI quantifies spatial patterns of degradation using von Neumann entropy, which inherently captures the same parameter interdependencies that are later modelled through the quantum density matrices in QPC. As such, the density matrix representation used in QEGWI becomes the foundational statistical structure leveraged by QPC for clustering. Moreover, the zones identified as Unsafe or Highly Unsafe by QEGWI largely align with high-entropy, high-risk clusters (C3, C4) in QPC, underscoring their interpretive consistency. Together, these models extend the traditional WQI framework from a deterministic to a probabilistic paradigm, enabling both parameter-specific insight and region-specific classification under spatial and statistical uncertainty. This integration enhances the scientific robustness of groundwater assessment and provides a policy-ready tool for risk-based intervention planning.

The spatial distribution of QEGWI scores reveals critical insights into groundwater quality across the study region. Districts in the coastal zones like Puri, Bhadrak, Ganjam, and Kendrapara consistently exhibit high QEGWI values. These patterns align with known salinity intrusions and coastal aquifer stress, as well as intensive agricultural and industrial activities (Kushawaha et al., 2024; Naik et al., 2021, 2022). The western and tribal-dominated districts show comparatively lower QEGWI scores (Goswami & Rai, 2023), reflecting more pristine groundwater conditions due to lower population density and reduced anthropogenic intervention. These spatial gradients emphasize the importance of moving beyond simple classification schemes toward entropy-aware assessments that reflect local variability.

To validate the proposed methodology, we compared QEGWI against a classical Shannon entropy-based GWQI. Both indices revealed similar spatial patterns, with a strong Pearson correlation ($r > 0.95$) across districts. However, QEGWI demonstrated superior sensitivity in distinguishing borderline cases districts with moderate contamination levels that were misclassified by the Shannon-based method. The Bland–Altman analysis further confirmed that while both indices generally agree, the QEGWI detected deviations in areas where subtle changes in parameter interdependence had meaningful implications on water quality classification. A confusion matrix analysis revealed higher precision and recall scores for QEGWI-based classification, strengthening the case for adopting von Neumann entropy in quality assessment.

Table.4 Confusion matrix comparing QEGWI and SE_GWQI classifications.

	QEGWI: Very Safe	QEGWI: Safe	QEGWI: Moderate	QEGWI: Unsafe	QEGWI: Highly Unsafe
SEGWI: Very Safe	0	0	0	0	0
SEGWI: Safe	0	269	1	0	0
SEGWI: Moderate	0	16	890	16	0
SEGWI: Unsafe	0	0	7	199	4
SEGWI: Highly Unsafe	0	0	0	0	38

Understanding uncertainty in environmental assessments is crucial for informed policy design. Monte Carlo simulations, based on parameter-specific standard deviations, allowed for the construction of confidence intervals around QEGWI scores. Most districts exhibited low uncertainty, reflecting stable groundwater chemistry; however, uncertainty was elevated in coastal districts such as Jagatsinghpur and Kendrapara, likely due to tidal fluctuations and salinity ingress.

Sensitivity analysis using Sobol indices, Pearson correlation coefficients, and standardized regression coefficients consistently identified Electrical Conductivity (EC), Sodium (Na^+), and Sulfate (SO_4^{2-}) as the most influential parameters driving QEGWI variability. These parameters not only serve as proxies for salinity and industrial contamination but also indicate vulnerability to both natural and anthropogenic stressors. The triangulation of multiple sensitivity measures enhances the robustness of parameter prioritization in future monitoring frameworks.

To complement the entropy-based index, we implemented QPC to delineate spatial clusters of groundwater quality under uncertainty. Unlike traditional clustering algorithms, QPC leverages quantum fidelity as a similarity measure and operates within a Hilbert space framework. This allows for probabilistic, non-binary membership, which is especially valuable in regions where water quality transitions are gradual rather than abrupt.

The QPC algorithm identified four distinct clusters. Cluster 0, comprising districts such as Koraput and Kandhamal, was characterized by low QEGWI and low entropy indicative of recharge-dominated zones with stable, high-quality groundwater. In contrast, Cluster 3, comprising Bhadrak, Angul, and parts of Ganjam, exhibited high entropy and high QEGWI, denoting zones of acute contamination with complex, uncertain parameter interactions. Clusters 1 and 2 represented transitional zones with moderate contamination and variable entropy, often located in physiographically complex regions. The probabilistic nature of QPC allows for overlapping memberships, reflecting the fuzzy and often indeterminate nature of hydro chemical boundaries in real aquifers.

Quantum fidelity scores between cluster centres reinforced the uniqueness of each group. Cluster 0 had the lowest similarity to Cluster 3, confirming that high- and low-risk zones are statistically and structurally distinct. The ability of QPC to represent gradual transitions rather than rigid partitions is particularly relevant for groundwater risk mapping, where administrative boundaries rarely coincide with hydrogeological ones.

Although rooted in quantum information theory, the application of quantum principles in this study is entirely statistical. The density matrix captures joint probability distributions across parameters, extending beyond classical variance–covariance matrices. Von Neumann entropy, as used here, serves as a multidimensional uncertainty measure rather than a physical quantum property. Similarly, quantum fidelity measures similarity between parameter distributions, enabling soft clustering through the QEM (Quantum Expectation Maximization) algorithm. These constructs allow the modelling of hydrogeochemical variability within a probabilistic framework, aligning with real-world groundwater systems where parameter interactions are rarely linear or independent.

This conceptual shift from deterministic scores to probabilistic, entropy-informed assessments enhances the interpretive power of groundwater quality indices. It also provides a scalable foundation for future work integrating quantum kernels, fuzzy logic, and Bayesian inference in groundwater modelling.

The dual framework of QEGWI and QPC offers actionable insights for groundwater governance. First, the entropy-weighted QEGWI can inform parameter prioritization in groundwater quality monitoring, guiding targeted remediation efforts in high-risk districts. Second, the probabilistic cluster zones can be directly mapped onto existing administrative or hydrogeological units to support district-wise intervention planning. For instance, Cluster 3 districts should be prioritized for salinity mitigation and stricter industrial discharge regulations, while Cluster 0 regions may focus on groundwater conservation and recharge.

Moreover, the QPC framework can be integrated into national groundwater mapping programs such as NAQUIM or Jal Shakti initiatives, offering a scientifically grounded method for dynamic risk zoning. As India scales its groundwater sustainability efforts, tools that capture uncertainty and parameter interactions will be increasingly vital for evidence-based policymaking.

While the study offers a robust and novel framework, several limitations merit attention. First, the temporal averaging of groundwater quality parameters may obscure seasonal variability. Future studies should incorporate seasonal datasets to capture dynamic trends and recharge effects. Second, the 1 km spatial resolution used for interpolation may introduce artifacts in data-scarce regions, particularly in interior Odisha. Third, although QPC accommodates uncertainty, it does not currently integrate external drivers such as land use, rainfall, or socio-economic variables.

Future work should explore the integration of spatio-temporal entropy with land use change models, as well as the use of quantum machine learning techniques to further enhance classification under uncertainty. Expanding the framework to other regions with differing hydrogeochemical profiles would also help assess the method's generalizability and policy relevance.

5. CONCLUSION

This study presents a novel quantum entropy-driven framework for groundwater quality assessment by integrating von Neumann entropy-based weight estimation and quantum probabilistic clustering (QPC) into groundwater monitoring and risk zoning. The proposed Quantum Entropy-based Groundwater Quality Index (QEGWI) successfully captures multivariate uncertainty, inter-parameter dependencies, and spatial variability that traditional WQI models and Shannon entropy-based methods fail to address.

QEGWI consistently identified fluoride (F^-), sodium (Na^+), and total dissolved solids (TDS) as dominant contributors to groundwater degradation across the region. Sensitivity analysis using first-order Sobol indices confirmed F^- and Na^+ as the most influential parameters (indices >0.35), highlighting their persistent role in regional water quality deterioration. Monte Carlo simulations ($n = 10,000$) revealed that QEGWI exhibits a narrower uncertainty spread (mean standard deviation ± 0.14) compared to the Shannon entropy-weighted WQI (± 0.23), confirming its robustness and stability under input perturbations. Spatial analysis of QEGWI scores identified distinct high-risk zones, particularly in coastal and industrial regions, with

values exceeding 0.75, signalling unsafe groundwater conditions without prior treatment. The Quantum Probabilistic Clustering (QPC) approach successfully classified groundwater sites into five interpretable risk-based clusters (C0–C4), effectively distinguishing between high-risk zones, moderate-risk transitions, and low-risk areas. QPC fidelity analysis reported high intra-cluster similarity (mean fidelity >0.85), while boundary or transitional zones exhibited classification uncertainties above 0.25, indicating zones of potential regime shift and intervention priority. Comparative evaluation showed that QEGWI enhanced the detection of unsafe groundwater locations by 18% and reduced transitional zone misclassifications by 22% compared to the Shannon entropy-based WQI, validating its scientific and operational advantage. Importantly, QPC extended the analytical capacity of QEGWI by providing spatially explicit, probabilistic zoning of risk clusters.

These findings not only demonstrate the scientific rigor and practical value of the quantum entropy-based framework but also underscore its potential to significantly enhance groundwater quality monitoring systems, particularly in geochemically complex regions. The integration of probabilistic spatial classification further provides a critical advancement toward uncertainty-aware groundwater governance and management frameworks.

References:

- Abidi, J. H., Elzain, H. E., Sabarathinam, C., Selmane, T., Selvam, S., Farhat, B., & Senapathi, V. (2024). Evaluation of groundwater quality indices using multi-criteria decision-making techniques and a fuzzy logic model in an irrigated area. *Groundwater for Sustainable Development*, 25, 101122.
- Abu, M., Musah, R., & Zango, M. S. (2024). A combination of multivariate statistics and machine learning techniques in groundwater characterization and quality forecasting. *Geosystems and Geoenvironment*, 3(2), 100261.
- Ahmad, A. Y., Saleh, I. A., Balakrishnan, P., & Al-Ghouti, M. A. (2021). Comparison GIS-Based interpolation methods for mapping groundwater quality in the state of Qatar. *Groundwater for Sustainable Development*, 13, 100573.
- Ahmad, S., Umar, R., & Ahmad, I. (2024). Assessment of groundwater quality using Entropy-Weighted Quality Index (EWQI) and multivariate statistical techniques in Central Ganga plain, India. *Environment, Development and Sustainability*, 26(1), 1615–1643.
- Aïmeur, E., Brassard, G., & Gambs, S. (2013). Quantum speed-up for unsupervised learning. *Machine Learning*, 90, 261–287.
- Amiri, V., Rezaei, M., & Sohrabi, N. (2014). Groundwater quality assessment using entropy weighted water quality index (EWQI) in Lenjanat, Iran. *Environmental Earth Sciences*, 72, 3479–3490.
- Barbieri, M., Barberio, M. D., Banzato, F., Billi, A., Boschetti, T., Franchini, S., & Petitta, M. (2023). Climate change and its effect on groundwater quality. *Environmental Geochemistry and Health*, 45(4), 1133–1144.
- Dai, H., Quddoos, A., Naz, I., Batool, A., Yaseen, A., Ali, M., & Alzahrani, H. (2025). Geospatial Decision Support System for Urban and Rural Aquifer Resilience: Integrating Remote Sensing-Based Rangeland Analysis With Groundwater Quality Assessment. *Rangeland Ecology & Management*, 99, 102–118.
- Das, A. (2024). Evaluation of surface water quality in Brahmani River Basin, Odisha (India), for drinking purposes using GIS-based WQIs, multivariate statistical techniques and semi-variogram models. *Innovative Infrastructure Solutions*, 9(12), 484.
- Dehghan Rahimabadi, P., Behnia, M., Nasabpour Molaei, S., Khosravi, H., & Azarnivand, H. (2024). Assessment of groundwater resources potential using Improved Water Quality

- Index (ImpWQI) and entropy-weighted TOPSIS model. *Sustainable Water Resources Management*, 10(1), 7.
- Dirac, P. A. M. (1981). *The principles of quantum mechanics* (Issue 27)).
- El Shinawi, A., Kuriqi, A., Zelenakova, M., Vranayova, Z., & Abd-Elaty, I. (2022). Land subsidence and environmental threats in coastal aquifers under sea level rise and over-pumping stress. *Journal of Hydrology*, 608, 127607.
- Giavarina, D. (2015). Understanding bland altman analysis. *Biochemia medica*, 25(2), 141–151.
- Goswami, S., & Rai, A. K. (2023). Impact of anthropogenic and land use pattern change on spatio-temporal variations of groundwater quality in Odisha, India. *Environ Sci Pollut Res*, 30, 101483–101500. <https://doi.org/10.1007/s11356-023-29372-1>
- Goswami, S., & Rai, A. K. (2024). Understanding the vulnerability of coastal groundwater aquifers in Odisha, India. *Environmental Earth Sciences*, 83(2), 44.
- Helton, J. C., & Davis, F. J. (2003). Latin hypercube sampling and the propagation of uncertainty in analyses of complex systems. *Reliability Engineering & System Safety*, 81(1), 23–69.
- Jena, M. R., Tripathy, J. K., Sahoo, D., & Sahu, P. (2024). Geochemical evaluation of groundwater quality in the coastal aquifers of Kujang Block, Jagatsinghpur District, Eastern Odisha, India. *Water, Air, & Soil Pollution*, 235(6), 349.
- Jha, P. K., & Tripathi, P. (2021). Arsenic and fluoride contamination in groundwater: A review of global scenarios with special reference to India. *Groundwater for Sustainable Development*, 13, 100576.
- Jozsa, R. (1994). Fidelity for mixed quantum states. *Journal of Modern Optics*, 41(12), 2315–2323.
- Judeh, T., Almasri, M. N., Shadeed, S. M., Bian, H., & Shahrour, I. (2022). Use of GIS, statistics and machine learning for groundwater quality management: Application to nitrate contamination. *Water Resources*, 49(3), 503–514.
- Karunanidhi, D., Raj, M. R. H., Roy, P. D., & Subramani, T. (2025). Integrated machine learning based groundwater quality prediction through groundwater quality index for drinking purposes in a semi-arid river basin of south India. *Environmental Geochemistry and Health*, 47(4), 119.
- Kisi, O., Azad, A., Kashi, H., Saeedian, A., Hashemi, S. A. A., & Ghorbani, S. (2019). Modeling groundwater quality parameters using hybrid neuro-fuzzy methods. *Water Resources Management*, 33, 847–861.

- Kushawaha, J., Nandimandalam, J. R., Madhav, S., & Singh, A. K. (2024). Evaluation of hydrogeochemical processes and saltwater intrusion in the coastal aquifers in the southern part of Puri District, Odisha, India. *Environmental Science and Pollution Research*, 31(28), 40324–40351.
- Loganathan, S., & Sathiyamoorthy, M. (2024). Assessing groundwater contamination risk in industrial zone of Ranipet district, Southern India: A modified DRASTIC and Fuzzy-AHP approach. *Results in Engineering*, 23, 102772.
- MacDonald, A. M., Bonsor, H. C., Ahmed, K. M., Burgess, W. G., Basharat, M., Calow, R. C., & Yadav, S. K. (2016). Groundwater quality and depletion in the Indo-Gangetic Basin mapped from in situ observations. *Nature Geoscience*, 9(10), 762–766.
- Mahanta, N., & Goswami, S. (2024). Groundwater vulnerability to fluoride pollution and health risk assessment in the western part of Odisha, India. *Environmental Science and Pollution Research*, 31(24), 35878–35896.
- Mir, I. A. (2025). Micronutrients and contaminants in the grazing and agricultural soils of Kashmir Valley, India. *Scientific Reports*, 15(1), 10949.
- Mohanty, A. K., & Rao, V. G. (2019). Hydrogeochemical, seawater intrusion and oxygen isotope studies on a coastal region in the Puri District of Odisha, India. *Catena*, 172, 558–571.
- Naik, M. R., Barik, M., Jha, V., Sahoo, S. K., & Sahoo, N. K. (2021). Spatial distribution and probabilistic health risk assessment of fluoride in groundwater of Angul district, Odisha, India. *Groundwater for Sustainable Development*, 14, 100604.
- Naik, M. R., Mahanty, B., Sahoo, S. K., Jha, V. N., & Sahoo, N. K. (2022). Assessment of groundwater geochemistry using multivariate water quality index and potential health risk in industrial belt of central Odisha, India. *Environmental Pollution*, 303, 119161.
- Neumann, J. (1955). *Mathematical foundations of quantum mechanics*. Princeton University Press.
- Nielsen, M. A., & Chuang, I. L. (2010). *Quantum computation and quantum information*. Cambridge university press.
- O'brien, R. M. (2007). A caution regarding rules of thumb for variance inflation factors. *Quality & Quantity*, 41, 673–690.
- Ojha, M., Goswami, S., Sahu, P. C., & Ojha, C. (2024). Identifying susceptible groundwater contamination zones in western Odisha of India using hydro-geochemical and geospatial approaches. *Journal of Contaminant Hydrology*, 261, 104302.

- Panday, D. P., Kumari, A., & Kumar, M. (2025). Alkalinity-salinity-sustainability: Decadal groundwater trends and its impact on agricultural water quality in the Indian Peninsula. *Science of The Total Environment*, 978, 179459.
- Patel, D., Pamidimukkala, P., & Chakraborty, D. (2024). Groundwater quality evaluation of Narmada district, Gujarat using principal component analysis. *Groundwater for Sustainable Development*, 24, 101050.
- Piper, A. M. (1944). A graphic procedure in the geochemical interpretation of water-analyses. *Eos, Transactions American Geophysical Union*, 25(6), 914–928.
- Rousseeuw, P. J. (1987). Silhouettes: A graphical aid to the interpretation and validation of cluster analysis. *Journal of Computational and Applied Mathematics*, 20, 53–65.
- Sahu, S., Gogoi, U., & Nayak, N. C. (2021). Groundwater solute chemistry, hydrogeochemical processes and fluoride contamination in phreatic aquifer of Odisha, India. *Geoscience Frontiers*, 12(3), 101093.
- Salh, Y. H. M., Su, C., Iqbal, J., Usman, U. S., Yousif, M. H., & Ismail, O. (2025). Hydrogeochemical processes regulating groundwater quality and its suitability for drinking purposes in the recent alluvial plain, Blue Nile Region, Sudan. *Environmental Geochemistry and Health*, 47(4), 1–23.
- Sany, S. R., Deb, S. R., Ahmed, F., Al Nayem, M. A., Ashikuzzaman, A. K. M., & Al Numanbakth, M. A. (2025). Evaluation of groundwater quality and potential health risks in the Tengrila Gas Field Blowout Region, Bangladesh: An in-depth analysis utilizing multivariate statistics, heavy metal indices and Monte Carlo simulation. *Journal of Hazardous Materials*, 490, 137744.
- Sartirana, D., Zanotti, C., Palazzi, A., Pietrini, I., Frattini, P., Franzetti, A., & Rotiroti, M. (2025). Assessing data variability in groundwater quality monitoring of contaminated sites through factor analysis and multiple linear regression models. *Journal of Contaminant Hydrology*, 269, 104471.
- Scanlon, B. R., Fakhreddine, S., Rateb, A., Graaf, I., Famiglietti, J., Gleeson, T., & Zheng, C. (2023). Global water resources and the role of groundwater in a resilient water future. *Nature Reviews Earth & Environment*, 4(2), 87–101.
- Singha, S., Pasupuleti, S., Singha, S. S., Singh, R., & Kumar, S. (2021). Prediction of groundwater quality using efficient machine learning technique. *Chemosphere*, 276, 130265.
- Sobol, I. M. (2001). Global sensitivity indices for nonlinear mathematical models and their Monte Carlo estimates. *Mathematics and Computers in Simulation*, 55(1–3), 271–280.

- Sridhar, D., & Parimalarenganayaki, S. (2024). Assessment of groundwater quality under unplanned urban environment: A Case Study From Vellore City, Tamilnadu, India. *Water, Air, & Soil Pollution*, 235(12), 1–25.
- Srivastava, M. K., Gaur, S., & Ohri, A. (2024). Analysing the Effectiveness of MCDM and Integrated Weighting Approaches in Groundwater Quality Index Development. *Water Conservation Science and Engineering*, 9(2), 35.
- Thanh, N. N., Chotpantarat, S., Ngu, N. H., Thunyawatcharakul, P., & Kaewdum, N. (2024). Integrating machine learning models with cross-validation and bootstrapping for evaluating groundwater quality in Kanchanaburi province, Thailand. *Environmental Research*, 252, 118952.
- Uddin, M. G., Rahman, A., Taghikhah, F. R., & Olbert, A. I. (2024). Data-driven evolution of water quality models: An in-depth investigation of innovative outlier detection approaches-A case study of Irish Water Quality Index (IEWQI) model. *Water Research*, 255, 121499.
- Vesković, J., Deršek-Timotić, I., Lučić, M., Miletić, A., Đolić, M., Ražić, S., & Onjia, A. (2024). Entropy-weighted water quality index, hydrogeochemistry, and Monte Carlo simulation of source-specific health risks of groundwater in the Morava River plain (Serbia). *Marine Pollution Bulletin*, 201, 116277.
- Zare, M. S., Nikoo, M. R., Al-Rawas, G., Al-Wardy, M., Nazari, R., Karimi, M., & Gandomi, A. H. (2025). Integrating machine learning and data envelopment analysis for reliable reservoir water quality index assessment considering uncertainty. *Hydrological Sciences Journal*, 1–16.
- Zhang, M., Wang, L., Zhao, Q., Wang, J., & Sun, Y. (2024). Hydrogeochemical and anthropogenic controls on quality and quantitative source-specific risks of groundwater in a resource-based area with intensive industrial and agricultural activities. *Journal of Cleaner Production*, 440, 140911.